Characterisation of the interaction between rat Pyruvate Dehydrogenase Kinase 4 and ADP

Thandeka Khoza

A dissertation submitted to the Faculty of Science, University of the Witwatersrand, Johannesburg, in fulfilment of the requirements for the degree of Masters of Science

Johannesburg, 2008

Declaration

I declare that the dissertation being submitted is my own, unaided work which is being submitted for the Degree of Master of Science at the University of the Witwatersrand, Johannesburg. It has not been submitted before for any degree or examination in any other University.

Signed by _____

_____ day of _____2008

Abstract

The primary role of pyruvate dehydrogenase kinase (PDK) is to regulate the activity of pyruvate dehydrogenase complex (PDC) with respect to the metabolic clearance of glucose via a phosphorylation mechanism. Therefore, inhibition of PDK is predicted to be important in the treatment of diabetes. ADP binds to the active site of PDK; and has been shown to inhibit PDK activity. This research work was aimed at studying one of the isoforms of PDK, specifically the rodent form, PDK4 (rPDK4) and further elucidating the binding properties of ADP to rPDK4.

The hypothetical structure of rPDK4 was modelled based on the coordinates of the published rPDK2 structure. The overall structural topology of rPDK2 appears to be preserved in rPDK4. Further, the ADP binding site between rPDK2 and rPDK4 was conserved at both the primary and tertiary level, and this suggested the mechanism of ADP binding to rPDK2 would be similar to that of rPDK4.

A histidine tagged-rPDK4 protein was expressed and purified using affinity and gel filtration chromatography. It was determined to be a homodimer (97 kDa) comprising two identical subunits. The rPDK4 protein was further identified to be rPDK4 using Western blot analysis as it reacted positively with an anti-rPDK4 monoclonal antibody. The purified rPDK4 protein contained kinase activity since it was able to undergo autophosphorylation and subsequently phosphorylate a peptide that contained the E1α subunit sites that are known to be phosphorylated by PDKs. The structure of rPDK4 protein was also characterised using circular dichroism and fluorescence spectroscopy.

The spectroscopic data of rPDK4 was consistent with published data on the structure of rPDK4.

The binding of ADP and ATP was studied using fluorescence quenching as both these ligands quench the intrinsic tryptophan fluorescence of rPDK4. The dissociation constant (K_d) values for ADP and ATP were determined to be 37 and 17.4 μM, respectively. The moderate affinity binding of ATP will greatly favour the exchange of ADP for a molecule of ATP to prevent PDK inhibition by ADP.

Acknowledgements

I would like to thank my supervisors Prof. H Dirr and Dr L Shoba-Zikhali for their guidance and support during the course of this study. I am also thankful to CSIR Biosciences for their financial assistance.

I am most grateful to my fiancé Duncan Sibiya for his love, patience, encouragement, support and being wonderful friend through this study. I am also thankful to my son Sakhanya Sibiya for being a good baby when mommy had to work long late nights.

My thank you is also extended to following people for walking this walk by my side: Lindiwe Nkabinbe, Phiyani Lebea, Fritha Hennessy, Neeresh Rohitlall, Justin Joordan, Joni Frederick, Varsha Chhiba, Kholiwe Ntlabati, Lyndon Oldfield, Robin Roth, Sani Gumede and members of Protein Structure-Function Research Unit at WITS University.

Lastly, I am extremely appreciative to my family; Dad, Mom, sisi Thule, buthi Mzi, Mhlengi, Siyathokoza (advocate Khoza to be), Sandile and Sanele for their love, support and giving me strength to work towards my aspiration.

Table of Contents

List of Figures

List of Tables

List of Abbreviations

ADP	Adenosine diphosphate
ATP	Adenosine triphosphate
ATPase	Adenosine triphosphate synthase
BCKDK	Branched-chained α-ketoacid dehydrogenase kinase
CD	Circular dichroism
CheA	Chemotaxis protein CheA
DCA	Dichloroacetate
DTT	Dithiothreitol
E1	Pyruvate decarboxylase subunit of pyruvate dehydrogenase kinase
E2	Dihydrolipoamide acetyltransferase subunit of pyruvate dehydrogenase kinase
E3	Dihydrolipo-amide dehydrogenase subunit of pyruvate dehydrogenase kinase
E3Bp	E3 binding protein
EnzV	Transmembrane histidine kinase
HPLC	High pressure liquid chromatography
HPt	Histidine phosphoryl-transfer
Hsp 90	Heat shock protein of 90 kDa
IPTG	Isopropyl-β-D-thiogalactopyranoside
kDa	kilodalton
K_d	Dissociation constant
LB	Luria-Bertani
mPKs	Mitochondrial protein kinase

NAD^+	Nicotinamide adenine dinucleotide
NADH	Nicotinamide adenine dinucleotide (reduced form)
OD	Optical density
PCR	Polymerase chain reaction
PDC	Pyruvate dehydrogenase complex
PDK	Pyruvate dehydrogenase kinase
PDP	Pyruvate dehydrogenase phosphatase
SDS-PAGE	Sodium dodecyl sulphate-polyacrylamide gel electrophoresis
SE HPLC	Size exclusion–high performance liquid chromatography
T2DM	Type 2 non-insulin dependent diabetes mellitus
TCA	Tricarboxylic acid cycle
α	Alpha
β	Beta
n_H	Hill constant

1 Introduction

1.1 Diabetes mellitus

Type 2 diabetes mellitus (non-insulin dependent diabetes mellitus; T2DM) affects 6 % of the modern society and this statistic is expected to grow annually by 6 % world wide (Korc, 2003; Kopelman and Hitman, 1998; Amos *et al.,* 1997). Diabetes results from the lack of synthesis of insulin, whose primary biological function is to regulate and maintain glucose homeostasis. Insulin resistance and obesity have been reported as risk factors for the development of T2DM (Kahn and Flier, 2000). During insulin resistance, cells involved in glucose metabolism such as adipose tissue, skeletal muscle and liver, are unable to respond to insulin signalling, thus resulting in high glucose levels in the blood.

1.2 Glucose regulation

Glucose is obtained from dietary carbohydrate and gluconeogenesis and its level in the body is tightly regulated. Gluconeogenesis primarily occurs in the liver and to a lesser extent in the kidney (Coleman *et al*., 1992). During gluconeogenesis, glucose is synthesised from non-carbohydrate precursors (pyruvate, lactate and glucogenic amino acids) as well as the breakdown of glycogen. Glycolysis ensures that the glucose is cleared from the blood and utilized as energy. Insulin is the primary hormone that mediates glucose clearance (Hawkes and Kar, 2002). Insulin binds to its receptor and induces a signalling cascade (Whitehead *et al*., 2000) that results in the transportation of glucose into the cell by glucose transporter protein (Glut4) (Zierath *et al*., 1996), as well as activation of enzymes that are involved in the glycolytic pathway and suppression of

gluconeogenesis. Under normal physiological conditions, glucose is metabolised to pyruvate in the cytosol. Pyruvate is then transported by pyruvate binding protein into mitochondria where it is metabolised into acetyl-CoA (Figure 1). The acetyl-CoA can be used in fatty acid synthesis in the cytosol or directly fed into the TCA cycle in the mitochondria (Randle, 1986 and Figure 1).

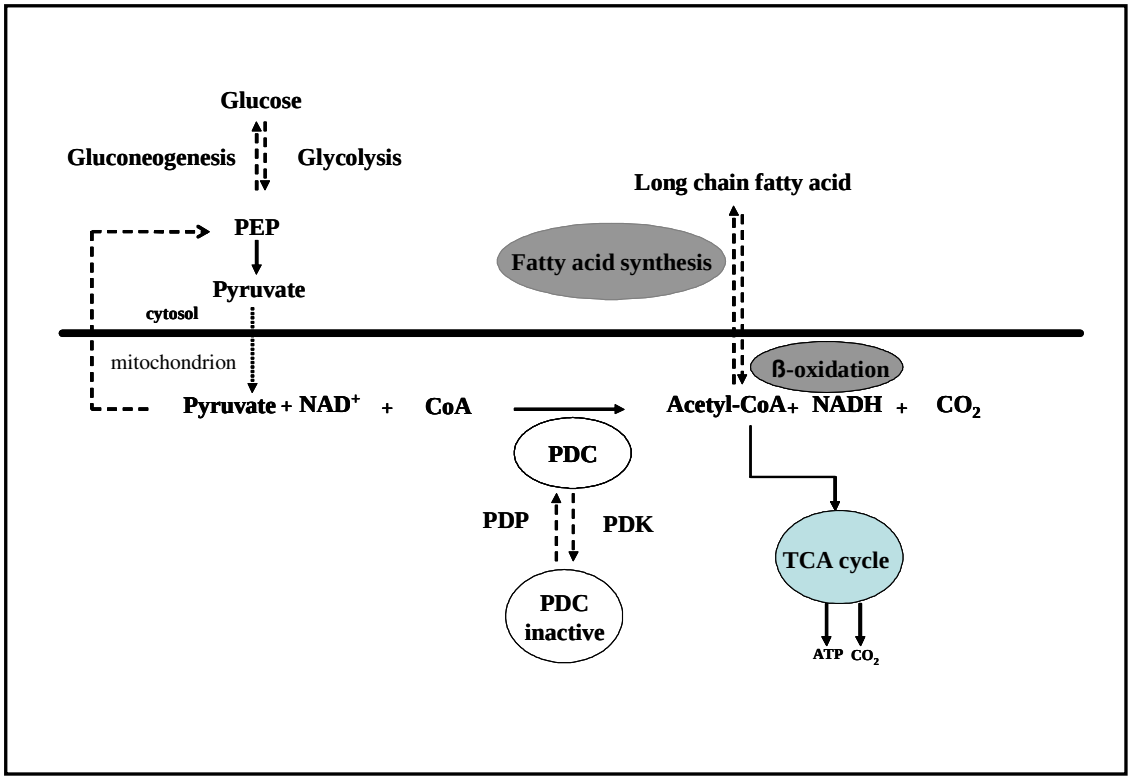

Figure 1: Schematic diagram showing the role of PDC in the clearance of glucose.

The link between glucose metabolism (in the cytosol), the TCA cycle (mitochondrion), and lipid synthesis cytosol is shown. The reaction catalysed by PDC is also shown. The positive regulator of PDC (pyruvate dehydrogenase phosphatase, PDP) is shown on the left, and the negative regulator (pyruvate dehydrogenase kinase, PDK) is shown on the right (Adapted from Patel and Korochkina, 2001).

1.3 Role of pyruvate dehydrogenase complex in glucose metabolism

The conversion of pyruvate to acetyl-CoA is irreversible and is catalysed by the pyruvate dehydrogenase complex (PDC), which is located in the matrix of mitochondria (Randle, 1986). PDC plays an important role in dictating the rate at which carbohydrate-derived substrates will be fully oxidized in tissues with large energy demands such as brain, muscle, heart and liver (Randle, 1986), thus contributing to the maintenance of glucose homeostasis (Randle, 1986; Patel and Roche, 1990). Consistent with this observation, the activity of PDC has been reported to be low during conditions of reduced glucose metabolism such as obesity, starvation and diabetes (Wieland *et al.,* 1971; Denyer *et al.,* 1981 and Henry *et al.,* 1991).

PDC is a multi-enzyme complex that is found in the mitochondria (Patel and Roche 1990; Reed *et al.,* 1985). It is composed of multiple copies of four different subunits (Patel and Roche 1990; Reed *et al.,* 1985) that include three catalytic enzymes (pyruvate dehydrogenase (E1), Dihydrolipoamide acetyltransferase (E2), and Dihydrolipoamide dehydrogenase (E3)), two regulatory enzymes (pyruvate dehydrogenase kinase (PDK) and pyruvate dehydrogenase phosphatase (PDP)), and E3 binding protein (E3Bp) (Patel and Roche 1990). E1 is made up of E1α and E1β subunits; the E1α has pyruvate dehydrogenase activity, and is responsible for the decarboxylation of pyruvate. The E2 subunit is responsible for the transfer of acetyl group to CoA while the E3 subunit transfers electrons to NAD^+ forming NADH (Patel and Roche 1990).

PDC catalyses the oxidative decarboxylation of pyruvate, and links glycolysis to the tricarboxylic acid cycle and ATP production (Figure 1). The efficiency of PDC is crucial

in tissues with a high ATP requirement and in lipogenic tissue (providing acetyl CoA for fatty acid synthesis). In an event where glucose is scarce, suppression of PDC is crucial. PDC is highly regulated due to the role that it plays in glucose homeostasis.

1.4 Regulation of PDC

PDC is regulated *via* both short-term and long-term mechanisms. The regulation of PDC within a few minutes to hours is termed short-term regulation, while regulation that occurs at transcriptional level within days to weeks is long-term (Patel and Korotchkina, 2001). With respect to maintenance of glucose homeostasis especially during transition between the fed and fasted states, PDC regulation *via* the short-term mechanism is highly critical. In the short-term mechanism, the E1 subunit of PDC is inactivated through phosphorylation by PDK, and reactivated *via* dephosphorylation by PDP (Yeaman *et al.,* 1978; Teague *et al.,* 1979; Hucho *et al.,* 1972 and Figure 2). PDK phosphorylates the E1α subunit of PDC on serine residues that are located on three different sites. These are designated site 1 (Ser^{264}), site 2 (Ser^{271}) and site 3 (Ser^{203}) (Sale and Randle, 1981). Korochkina and Patel (1995) constructed E1α mutants by converting the serine residues at different phosphorylation sites to alanine, leaving only one functional phosphorylation site at a time. They reported that phosphorylation of each site alone results in the complete inactivation of PDC (Yeaman *et al.,* 1978; Dahl *et al.,* 1987; Korotchkina and Patel, 1995). These sites are believed to define PDK species specificity.

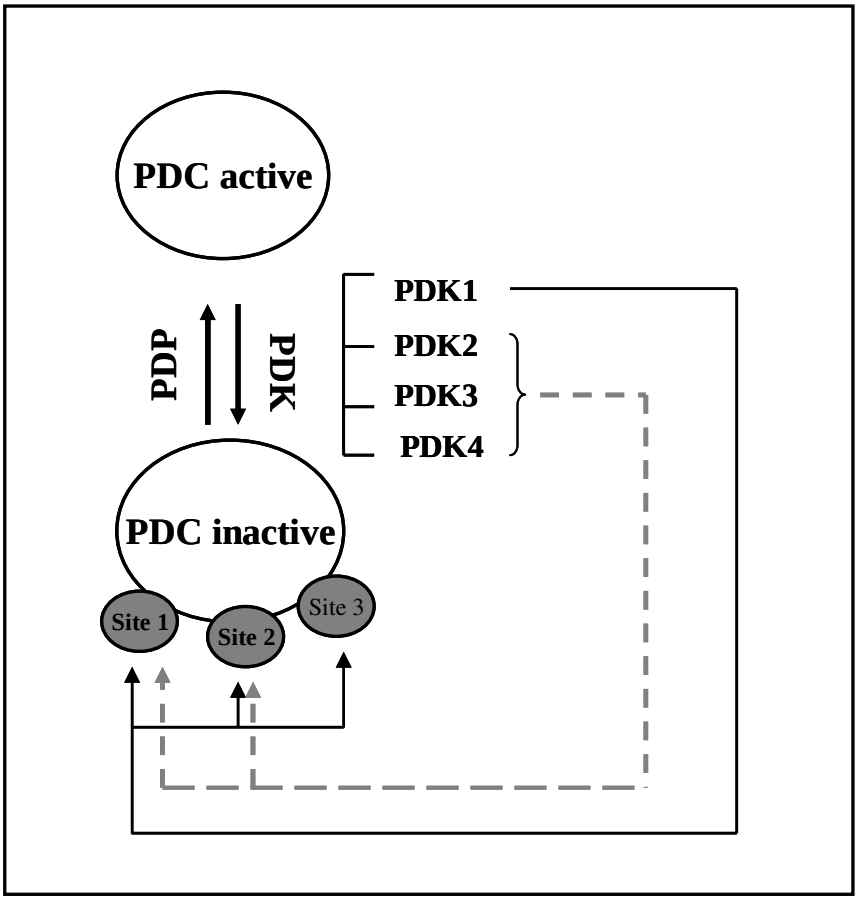

Figure 2: Regulation of PDC activity by a phosphorylation-dephosphorylation cycle.

To date, four isomers of PDK have been identified and cloned. These are PDK1 (Popov *et al.,* 1993), PDK2 (Popov *et al.,* 1994), PDK3 (Gudi *et al.,* 1995) and PDK4 (Rowles *et al.,* 1996). All four isomers have been shown to be capable of phosphorylating PDC *in vitro*. However, the relative catalytic activity of the PDK isozymes towards the E1 subunit of PDC varies, with PDK2 having the highest activity, followed by PDK4, PDK1 and PDK3 (Bowler-Kinley *et al.,* 1998). Further, the relative specificities of the PDK isoforms towards the three phosphorylation sites of the E1 PDC subunit differ (Korotchkina and Patel, 2001). All PDK isoforms are capable of phosphorylating sites 1 and 2, and only PDK1 is able to phosphorylate site 3 (Figure 2). Site 1 has been proposed to be the primary site for inactivation of PDC since site 1 phosphorylation is the most rapid and it is specific to PDK1 (Korotchkina and Patel, 2001). PDK4 showed

highest activity towards site 2 when compared to the other isomers with PDK1, PDK2 and PDK3 (Korotchkina and Patel, 2001, Kolobova *et al*., 2001). The observation that the activation of PDC by PDP is much slower when site 2 is phosphorylated (Holness and Sugden, 1989) led to the hypothesis that the phosphorylation of site 2 is primarily for slowing down the rate of re-activation of PDC by PDP (Korotchkina and Patel, 2001).

PDC activity is also regulated through a feed back loop. For example, the products of PDC reaction (e.g. NADH and acetyl-CoA) inactivate PDC by increasing the activity of PDK (Cooper *et al.,* 1975; Holness and Sugden, 1989). PDC substrates (e.g., pyruvate and NAD^+) activate PDC by inhibiting PDK activity. This feedback loop is shown through schematics in Figure 1.

1.5 Regulation of PDK

As discussed above, PDK plays a critical role in glucose homeostasis by regulating PDC activity. Consistent with this role, PDK activity is also tightly regulated through long-term and short-term mechanisms (Siess and Wieland, 1976; Dennis *et al.,* 1978; Kerbey and Randle, 1982).

1.5.1 Long-term mechanism

The long term regulation of PDK occurs at the gene expression level and is believed to be a part of an adaptive response to conditions of decreased glucose utilization, and increased fatty acid oxidation (Randle, 1986). This state is induced by nutrition and hormonal changes (Wu *et al.,* 1998). For example, starvation (Wu *et al.,* 1998; Kolobova

et al., 2001; Sugden *et al.,* 1998), high fat feeding (Sugden *et al.,* 2000; Holness *et al.,* 2000) and diabetes (Sugden *et al.,* 1998; Holness *et al.,* 2000; Wu *et al.,* 1999) lead to high PDK4 expression. Hormones, such as insulin, have also been shown to regulate PDK levels by suppressing PDK gene expression (Huang *et al.*, 2000; Majer *et al.,* 1998). Glucocorticoids are also known to induce PDK4 expression (Huang *et al.*, 2000). However their mechanism of activation is not clearly understood.

1.5.2 Short-term mechanism

The short term regulation of PDK involves direct modification of its activity by the substrates (pyruvate, NAD^+, and CoA) and the products (NADH, and Acetyl-CoA) of the PDC reaction (Figure 1 and Figure 3). Pyruvate inhibits PDK activity by binding to an allosteric site on PDK (Pratt and Roche, 1979; Kato *et al.,* 2005). Furthermore, the effect of pyruvate to PDK is synergistic with the effect of ADP (Pratt and Roche, 1979). It is believed that the binding of pyruvate to the PDK-ADP complex results in conformational changes which prevent release of the ADP molecule from the active site of PDK. This ensures that the PDK remains in an inactive form (Kato *et al.,* 2005; Steussy *et al.,* 2001). NADH, and acetyl-CoA (Figure 1 and Figure 3) induce PDK activity (Ravidran *et al.,* 1996 and Bowker-Kinley *et al.,* 1998) by binding to the inner lipoyl domain (L2) of PDC.

1.6 Expression of PDK and its link to T2DM

PDK isoforms are expressed differently in different cell types (Bower-Kinley *et al*, 1998; Bowker-Kinley and Popov, 1999). The expression of PDK1 is limited to heart and pancreas (Bowker- Kinley and Popov, 1999; Sugden *et al.,* 2001; Wu *et al.,* 1999). PDK

2 is expressed with low amounts in the lung and spleen (Huang *et al.,* 1998), whereas PDK3 is found only in the testis, kidney and brain (Huang *et al.,* 1998; Bowker-Kinley and Popov, 1999). For example, the expression of PDK4 is found in the tissues that are important in the metabolic clearance of glucose such as liver and skeletal muscle (Bowker-Kinley and Popov, 1999; Sugden *et al.,* 2001; Wu *et al.,* 1999). This suggests that PDK4 is the critical isomer involved in the maintenance of glucose homeostasis. Consistent with this hypothesis, PDK4 is expressed in high levels during obesity and diabetes (Holness and Sugden, 1989; Kolobova *et al.*, 2001). In addition, an increase in PDK4 expression has been observed in response to starvation and insulin resistance

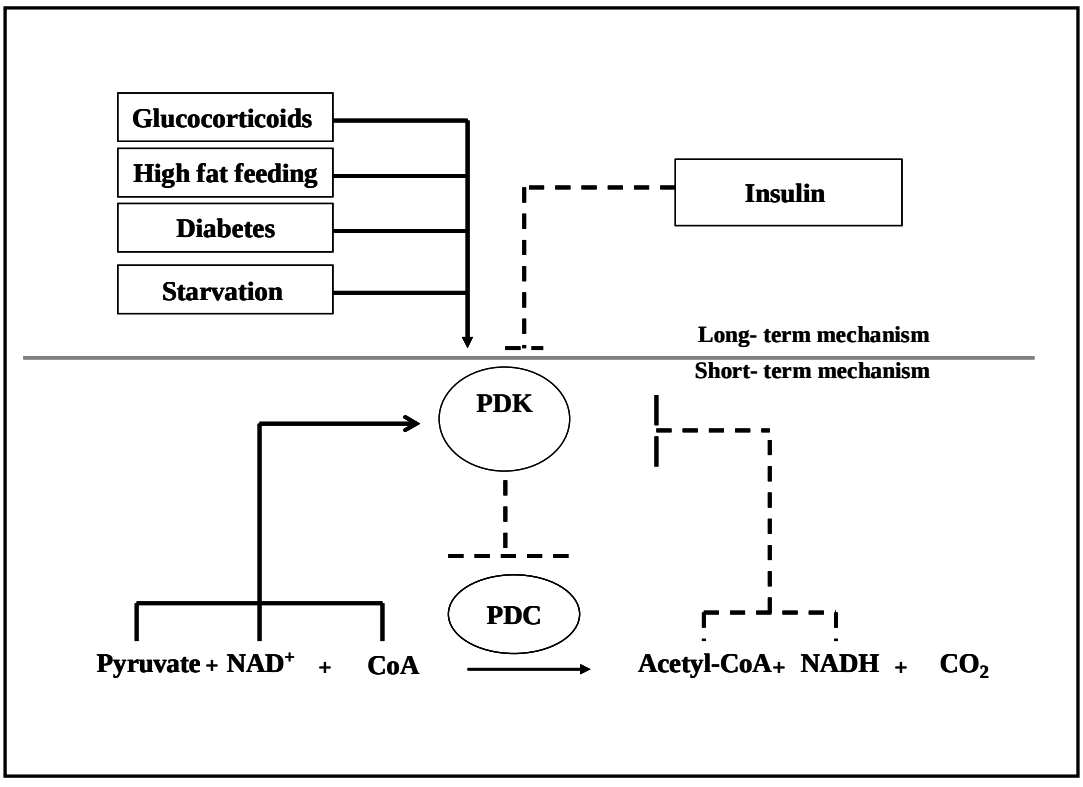

Figure 3: The long-term and short-term regulation of PDK.

The reaction catalysed by PDC is also shown. The arrows show factors that induce PDK expression and activity. The broken lines indicate factors that inhibit PDK expression and activity.

Taking into account that PDK4 shows high specificity towards site 2 of PDC, the increase of PDK4 levels in response to starvation, insulin resistance and diabetes is believed to be important for site 2 phosphorylation. It is postulated that phosphorylation of site 2 by PDK4 results in limiting the rate of PDP-dependent reactivation of PDC, thus ensuring that PDC remains in the inactive form. This postulate is supported by the observation that the reactivation of PDC in the heart, liver and skeletal muscle is much slower under conditions of high PDK4 expression than under conditions of low PDK4 expression (Holness and Sugden, 1989). Therefore, PDK4 seems to be an ideal target for long-term inhibition of PDK activity with respect to control of T2DM.

1.7 Classification of PDK

PDKs, together with branched-chained α-ketoacid dehydrogenase kinases (BCKDK), form a novel family of eukaryotic protein kinases, namely the mitochondrial protein kinases (mPKs) (Popov *et al.,* 1993; Davier *et al.,* 1995). These are serine specific protein kinases which share more similarity with prokaryotic protein kinases, despite being eukaryotic. PDKs belong to the ATPase/kinase superfamily which consists of bacterial histidine kinases (EnzV and CheA) and ATPases (Hsp90 and DNA Gyrase B) (Harris *et al.,* 1995), whereas eukaryotic protein kinases have a different molecular signature (Popov *et al*., 1993; Hanks and Hunter, 1995) that is depicted in Figure 4A. The catalytic subunit of eukaryotic serine/threonine kinases contains eight subdomains which play an essential role in the functioning of the enzyme through involvement in the binding and orientation of ATP, or the protein substrate. They also partake in the transfer

of the γ-phosphate from ATP to the acceptor hydroxyl residue (Ser, Thr or Tyr) of the protein substrate (Hanks and Hunter, 1995).

The PDK enzymes, despite being mammalian serine protein kinases, lack sequence motifs that are associated with eukaryotic serine/threonine kinases (Popov *et al.,* 1993), but show more similarity to prokaryotic histidine kinases (Popov *et al.,* 1993). The structural elements of PDKs which are also characteristic of histidine kinases have been defined by a number of researchers (Popov *et al.,* 1993; Steussy *et al.,* 2001 and Kato *et al.,* 2005). These are depicted in Figure 4B.

1.8 Structure of PDK

Primary sequence analysis of the PDK isomers shows that they contain a poorly conserved N-terminal domain and a highly conserved C-terminal domain (Figure 4B and Figure 5). Furthermore, PDK isomers exhibit high sequence similarity within the group (Figure 5). PDK isoforms show high sequence conservation among different eukaryotic species, for example rat and human PDK2 proteins share greater than 95 % identity in their primary amino acid sequence. The total number of amino acid residues varies among the different PDK isomers, for example PDK1 has 436 residues, PDK2 and PDK4 have 407 residues, and PDK3 has 406 residues (Rowels *et al.,* 1996; Figure 5). Similarly, the apparent molecular masses of the PDKs determined by polyacrylamide gel electrophoresis vary such that mature PDK1 corresponds to a 45 kDa subunit, whereas mature PDK2, PDK3, and PDK4 correspond to a 48 kDa subunit.

In the PDK family, PDK2 (Steussy *et al.,* 2001) and PDK3 (Kato *et al.,* 2005) are the only isomers with crystal structures that have been solved. PDKs are reported to be homodimers (Figure 6A) with each monomer folding into a well defined 45 kDa subunit (Figure 6; Steussy *et al.,* 2001; Kato *et al.,* 2005).

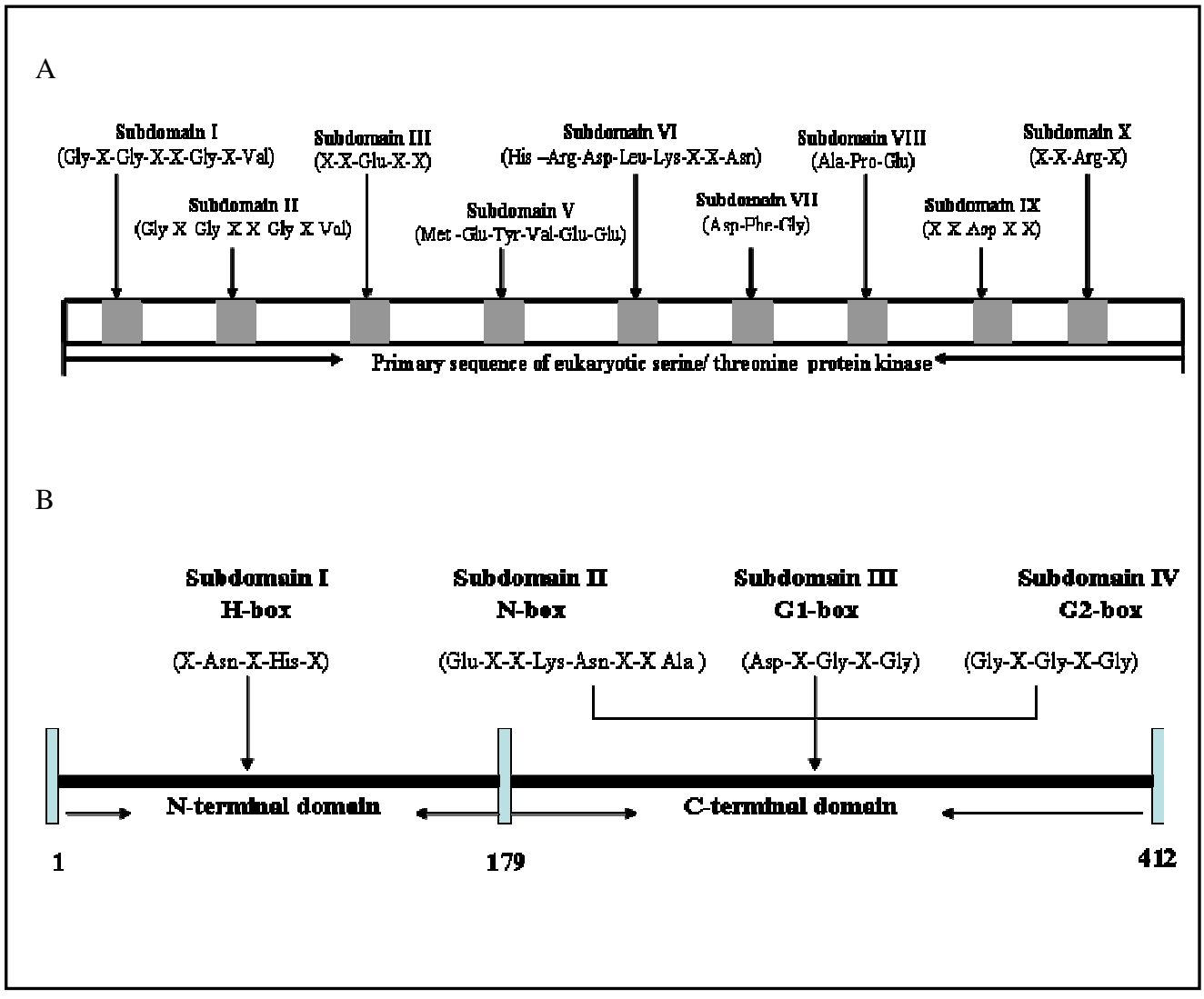

Figure 4: Comparison of the primary structure of eukaryotic serine/threonine kinases with that of the PDK family.

Primary structures of ATPase/kinase superfamily and of eukaryotic serine/threonine kinase are shown in Figure 4A (Hanks and Hunter, 1995) and 4B (Popov *et al.,* 1993), respectively. The conserved subdomains which are the signature regions of these kinases are depicted in the figure above.

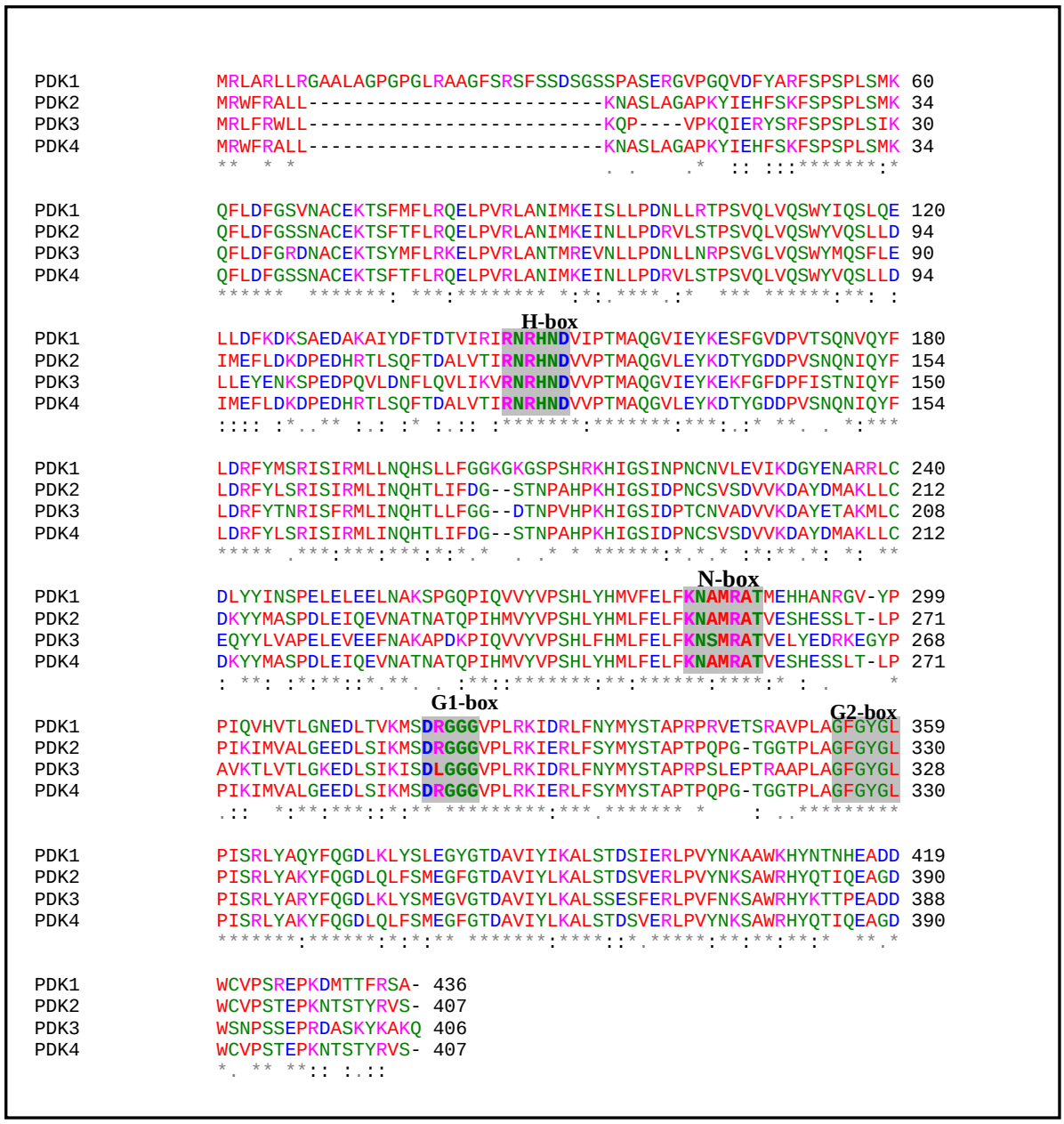

Figure 5: Multiple alignment of amino acid sequences of the rat PDK isoforms.

The sequences were aligned using ClustalW, version 1.83 (Thompson *et al.,* 1994). The sequence of the PDK isozymes were obtained from GenBank and their accession numbers are as follows: PDK1-Q15118, PDK2-Q64536, PDK3-Q15120, and PDK4- O54937. Colours indicate chemical properties of the specified amino acid residues; asterisks at the bottom of each sequence alignment indicate residues that are conserved among the different PDK proteins; the colon indicates amino acid substitution with conserved hydrophobicity or chemical properties; full stop indicates position where there are at least two amino acid conservations. Shaded regions indicate the subdomains that are conserved in the PDK family as well as bacterial histidine kinases. These are labelled above each conserved box.

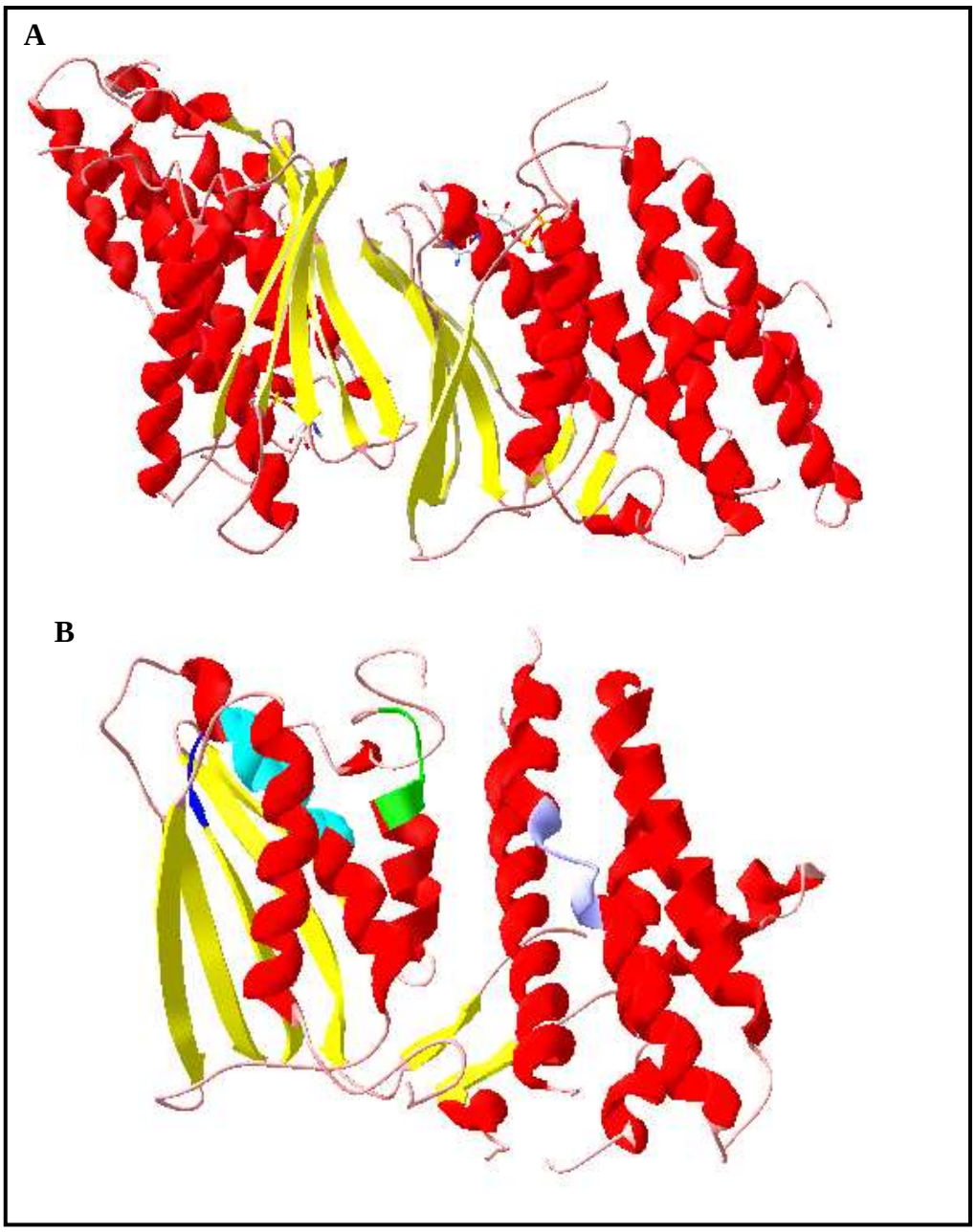

Figure 6: A ribbon representation of the structure of rat PDK2.

These images were generated using Swiss PDB Viewer (Guex and Peitsch, 1997) based on coordinates of 1JM6 (PDB code) published by Steussy *et al*. (2001). The dimer and monomer are shown in A and B, respectively. α-Helices are coloured in red, β-strands are coloured in yellow, and the loop regions are coloured in pink. In addition, the conserved subdomains are shown in the following colours: blue is G1 box, G2 box is green, N box is cyan and H- box is lilac.

The C-terminal domain is an α/β structure with five β strands (Figure 6). This fold resembles the one present in the ATPase/kinase superfamily such as CheA (Bilwes *et al.,* 1999), enzyme kinases (Tanaka *et al.,* 1998) and Hsp90 (Prodromou *et al.,* 1997). Furthermore, the C-terminal domain contains the three subdomains referred to as N- box (Glu-x-x-Lys-Asn-x-x-Ala), G1-box (Asp-x-Gly-x-Gly) and G2-box (Gly-x-Gly-x-Gly) (Popov *et al.,* 1993; Steussy *et al.,* 2001; Figure 5 and 6B). These subdomains are present throughout the ATPase/kinase superfamily.

The G-boxes contain glycine rich loops which are characteristic of nucleotide binding domains (Rossman *et al.,* 1974). Their nucleotide binding role was confirmed by resolving the structure of rat PDK2 that was crystallised with a bound molecule of ADP (Steussy *et al.,* 2001). The residues in the G1-box served as the basis of adenine specific interaction between ADP and the kinase. The G1-box is part of a loop connecting α helices 10 and 11, and it forms one side of the binding pocket with the G2-box forming the other side (Steussy *et al.,* 2001). The G-boxes together with the N-box serves as a unique ATP binding fold (Bergerat *et al.,* 1997 and Alex and Simon 1994) and an ATP lid (Machiuss *et al.,* 2001 and Kato *et al.*, 2005). The amino acids in the N-box play an important role in the activity of PDK.

The N-terminal domain is made up of eight α-helices connected by flexible loops and this domain begins at residue 1 and ends at residue 179. The N-terminal domain contains a conserved subdomain called an H-box (x-Asn-x-His-x-Asp) (Figure 5; Kim and Forst, 2001; Parkinson and Kofoid, 1992) which was initially predicted to be the site of autophosphorylation of PDK (Harris *et al.,* 1995). The α-helices form a four helix bundle that resembles the histidine phosphoryl-transfer (HPt) domain of the two-component

systems. In a two-component signal transduction pathway, a histidine kinase catalyses the first step where the sensor domain responds to a signal by autophosphorylation of a histidine residue within the transmitter domain. This is then relayed by transferring the phosphate group to an aspartic acid residue within the receiver domain of a cognate response regulator protein which is usually a transcription factor. However, in PDKs, the H-Box in the N-terminal domain was proved not to be the site of PDK autophosphorylation, since autophosphorylation was mapped to serine residues in this domain (Thelen *et al.,* 2000).

1.9 Reaction mechanism of PDK

At present, all studied and characterized histidine kinases transfer phosphate from an autophosphorylated histidine residue to an aspartate residue resulting in transduction of cellular signals. PDK contains two prototypical component histidine motifs (Popov *et al.,* 1993) and His^{115} was presumed to be a site of autophosphorylation and a phosphor-His catalytic intermediate in PDKs. Studies performed by Mooney and co-workers demonstrated that treatment of PDK by histidine modifying reagents diethyl pyrocarbonate and dichloro-(2,2':6',2'-terpyridine)-platinum (II) dihydrate completely abrogates PDK activity (Mooney *et al.,* 2000). This supported an essential role of His^{115} in PDK catalytic activity. This theory was later disproved by solving the crystal structure of rat PDK2 (Steussy *et al.,* 2001). The determination of the structure of rat PDK2 suggested that His^{115} is solvent inaccessible making it unlikely to partake in a phosphor-histidine intermediate. Furthermore, His^{115} plays an important role in making a number of crucial structural hydrogen bonds (Steussy *et al.*, 2001). Currently, the site of autophosphorylation of PDK is not clearly defined.

In attempt to decipher the reaction mechanism of PDK, Tuganova *et al.* (2001) and Tovar-Mendez *et al.* (2005) studied the roles of Leu^{234} and Glu^{238} which are located in the N –box. The mutation of these amino acid residues to alanine resulted in a complete loss of PDK activity. The asparagine and lysine residues which are also located in the N-box were found to interact directly with ATP (Steussy *et al.,* 2001). According to the rPDK2 structure, the lysine residue in the N-box is oriented towards the ATP binding site. It was therefore hypothesised that this lysine residue is involved in the catalysis of PDK. This hypothesis was strengthened by the low k_{cat} of PDK mutated at this lysine residue (Tovar-Mendez *et al.,* 2005).

Tovar-Mendez *et al.* (2005) proposed a model for the catalytic roles of amino acids in the N-box (Figure 7). In this model, the conserved amino acids of the N-box (Glu and Lys) participate in binding of Mg^{2+} *via* a water molecule that coordinates the Mg^{2+} with asparagine completing the magnesium octahedral sphere. The proposed role of Glu^{238} was strengthened by observing that, in the other members of the ATPase/kinase superfamily such as CheA and topoisomerase, the amino acids that correspond to Glu^{238} participate indirectly in the binding of Mg^{2+} *via* a water molecule that coordinates the Mg^{2+} (Bilwes *et al.,* 2001; Corbett and Berger, 2003). The base catalyst is proposed to be either located in the ATP lid or in the substrate.

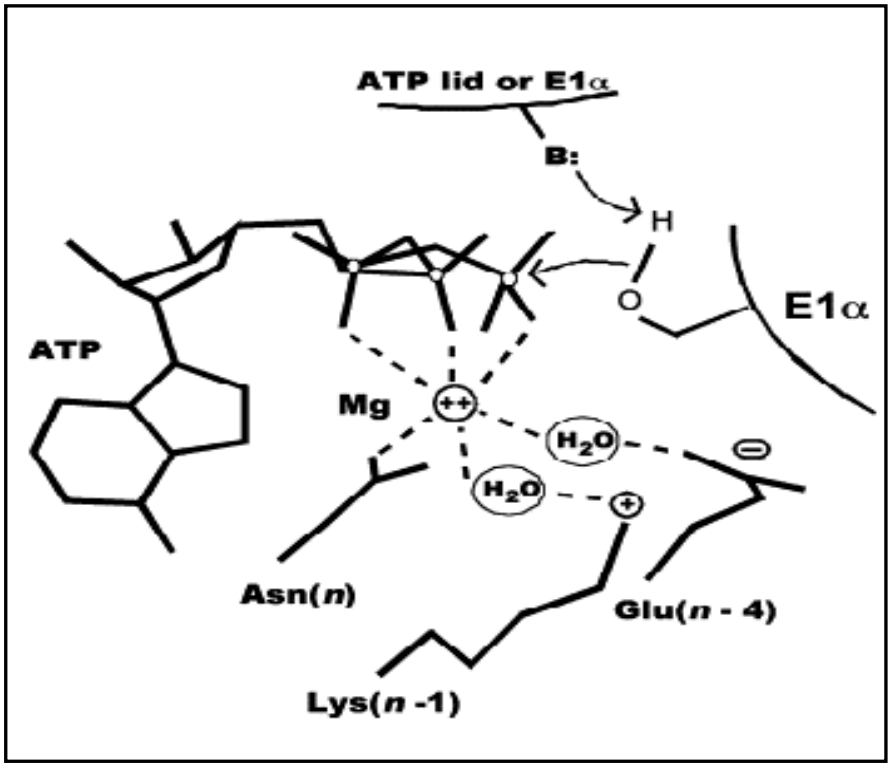

Figure 7: Proposed model for the roles of the amino acids in the N-box.

Dotted lines indicate the interaction between the amino acid residues and magnesium or water molecules. The water molecules bridge Mg^{2+} with Glu^{243} and Lys^{242}. The Asn^{242} is involved in the direct binding of Mg^{2+}. The two water molecules, Glu^{243}, Lys^{242} and Asn^{242} complete the magnesium octahedral sphere (taken from Tovar-Mendez *et al*., 2005).

1.10 Inhibitors of PDK

PDK has received attention as a target for T2DM therapy due to its role in glucose metabolism and diabetes. Therefore, there have been a number of efforts to identify or design PDK inhibitors. Currently, the only known inhibitor of PDK that has reached clinical trial stage is Dichloroacetate (DCA). Recently, other inhibitors of PDK activity such as triterpenes (Aicher *et al*., 1999), analogues of ATP, lactones and halogenated acetophane (Mann *et al*., 2000) have been identified (Figure 8). However, they have not yet reached clinical trial stage.

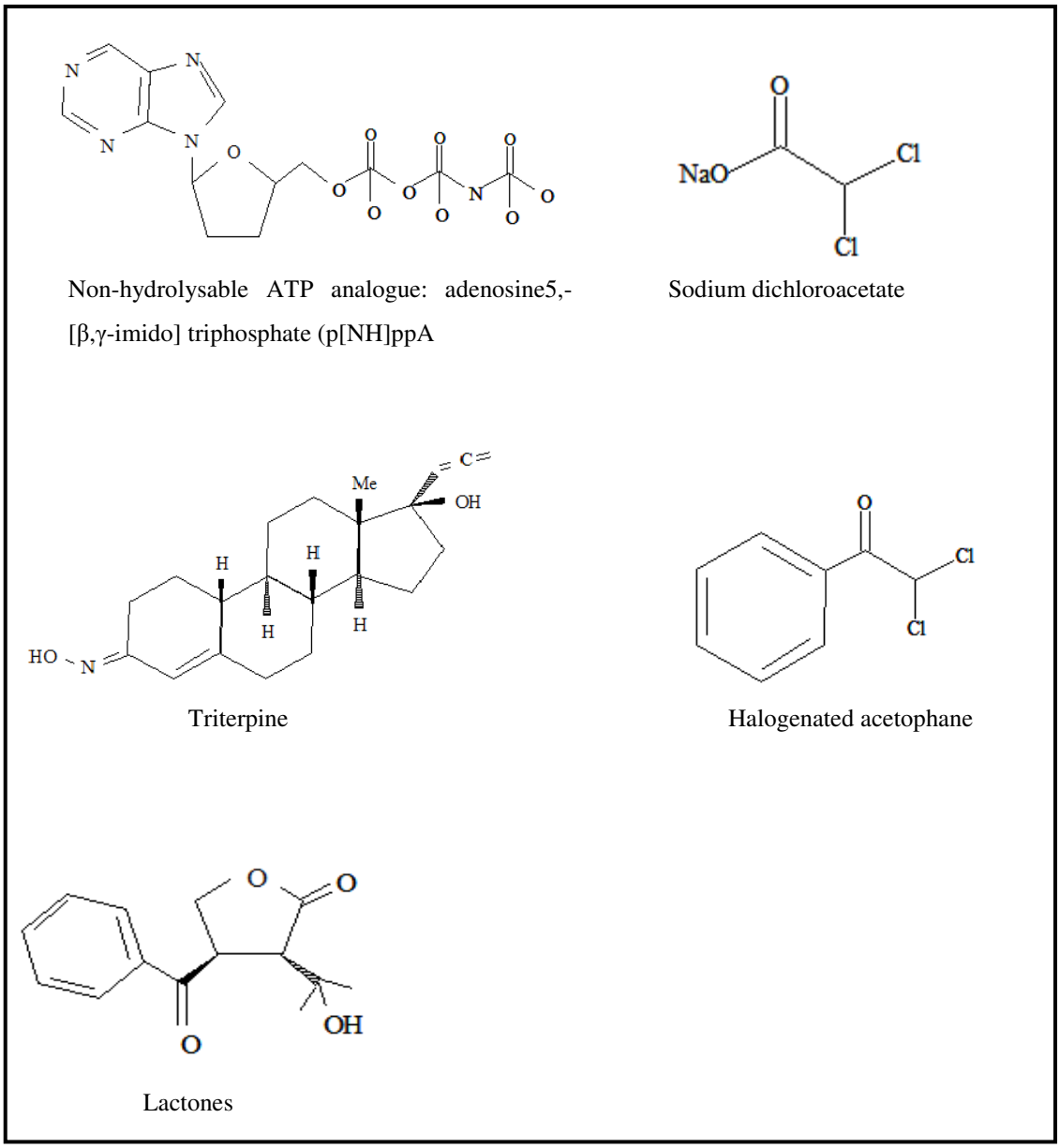

Figure 8: Structures of PDK inhibitors.

These structures were adapted from Mann *et al.* (2000).

1.10.1 DCA as a PDK inhibitor

DCA (Figure 8) is a non-hydrolysable analogue of pyruvate that has been shown to improve the diabetic condition (Whitehouse *et al.*, 1974 and Stacpoole *et al.*, 1979). In

addition, DCA has been used for other conditions in which PDC activity is reduced such as ischemia (Preiser *et al.,* 1990), and cardiac insufficiency (Bersin *et al.,* 1997).

DCA binds to PDK at an allosteric site that was mapped using the crystal structure of human PDK2 complexed to DCA (Knoechel *et al*., 2006). This site is located in the N-terminal domain and is formed by residues Leu^{53}, Tyr^{80}, Ser^{83}, Ile^{111}, Arg^{112}, His^{115}, Ser^{153}, Arg^{154}, Ile^{157}, Arg^{158} and Ile^{161} (Knoechel *et al*., 2006 and Figure 9). Most of these residues are conserved in all the known PDK isoforms (Figure 5). The carboxylate group of DCA forms a salt-bridge with Arg^{158} while the chlorine is buried in the hydrophobic portion of the DCA binding site (Knoechel *et al*., 2006). It is believed that binding of DCA to PDK prevents dissociation of ADP from the active site of PDK (Bao *et al*., 2004) thus locking PDK in its inactive form.

DCA has proved not to be ideal for long term treatment of T2DM due to its toxicity (Stacpoole *et al.,* 1979; Katz *et al.,* 1981; Toth *et al.,* 1992 and Yount *et al.,* 1982). The toxicity of DCA results from it being metabolized to glyoxylate which is converted to oxalate. High amounts of oxalate lead to abnormal oxalate metabolism (Stacpoole *et al.,* 1990). Furthermore, DCA stimulates thiamine-dependent enzymes which cause depletion of thiamine in the body (Stacpoole *et al.,* 1990). It is, therefore, imperative to investigate other useful drugs that can inhibit PDK activity for the therapy of diabetes and other metabolic disorders.

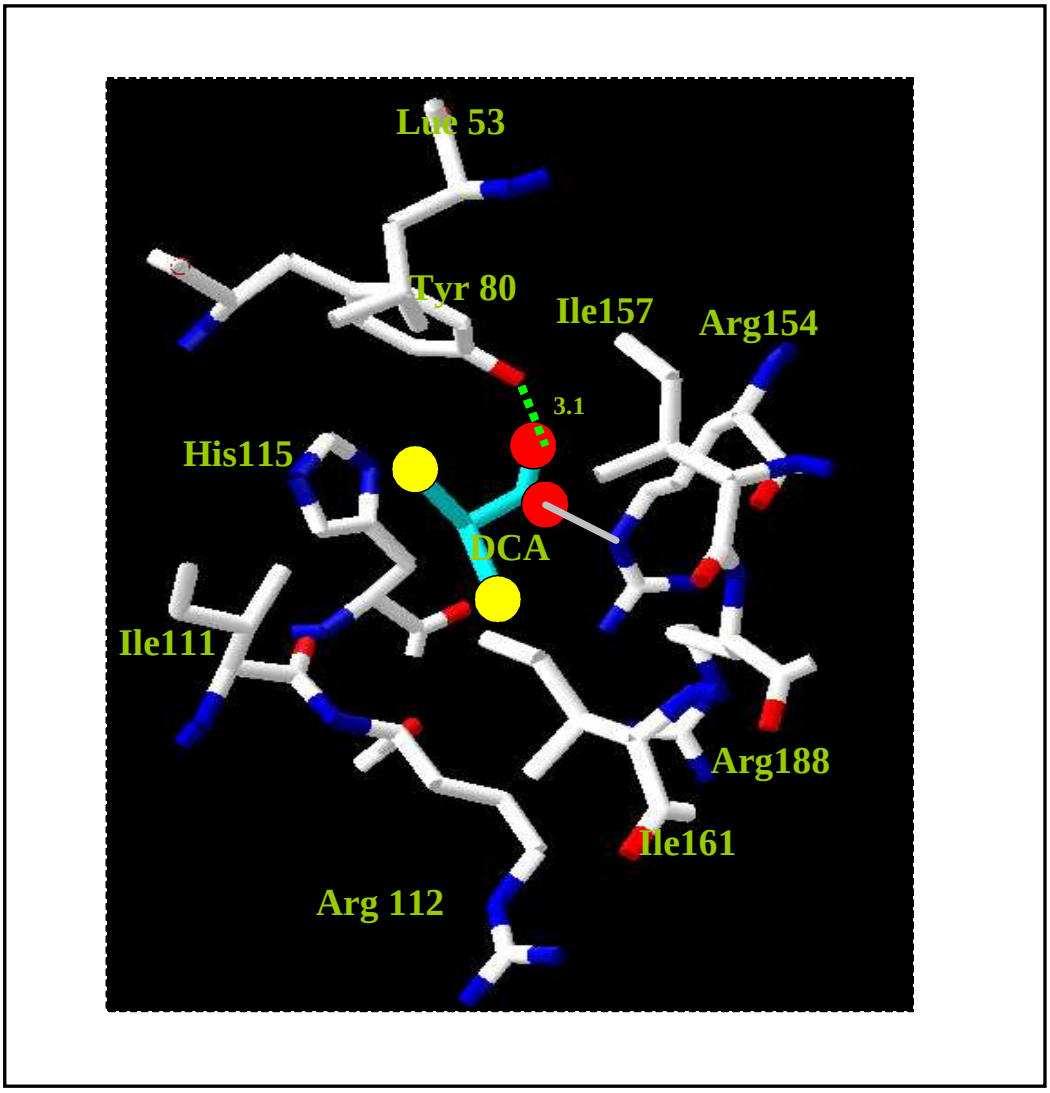

Figure 9: Interactions between DCA and the residues in the DCA binding site of PDK2.

The DCA allosteric pocket in PDK is coloured according to CPK colour scheme where red indicates region with negative charge, blue a positive charge region and white a neutral region. The DCA molecule is coloured cyan. The red and yellow rings in DCA molecule denote the oxygen and chlorine atoms, respectively. The green dotted line shows hydrogen bonds between DCA and Tyr^{80} while the solid grey line represents a salt bridge that is formed between Arg^{145} and DCA. This image was generated using Swiss PDB Viewer (Guex and Peitsch, 1997) based on coordinates of 2BU8 (PDB code) (Knoechel *et al.*, 2006).

1.10.2 Remarks on protein kinases as drug targets

Protein kinases have revealed themselves to be ideal targets for rationally designed inhibitory drugs. Through this process, a number of inhibitors have been synthesized and had successful outcomes in clinical trials. These inhibitors target different regions in the kinases, such as the nucleotide binding domain, the site of allosteric activation of the kinases, and the site of interaction between the kinase and other regulatory proteins. Examples of kinase inhibitors that bind the nucleotide domain include Iressa®, (Baker *et al.,* 2001) and staurosporine (Prade *et al.,* 1997). Iressa® binds irreversibly to the EGFR tyrosine kinase by covalently binding the cysteine in the ATP binding pocket, and staurosporine binds to the adenosine pocket of the catalytic subunit of cAMP-dependent protein kinase. These compounds are able to inhibit effectively the nucleotide binding site because it has a loop region that contains a conserved glycine-rich sequence. The glycine residues in this site make the loop region very flexible in the absence of ATP thus allowing binding of small molecule inhibitors (Mohammadi *et al.,* 1997; Huse and Kuriyan, 2002). These inhibitors induce structural changes thus preventing substrate binding (Mohammadi *et al.,* 1997).

However, as the nucleotide binding domains are ubiquitous, specificity is a concern. In attempts to address the specificity of kinase inhibitors, inactive forms of kinases are being targeted since they differ in structure (Noble *et al.,* 2004). This approach has been successfully employed in designing Gleevec, a specific inactive c-Abl kinase inhibitor (Nagar *et al.,* 2003). Gleevec acts by binding to the inactive form of c-Abl kinase thus locking the enzyme in its inactive conformation (Nagar *et al.,* 2003). An example of an inhibitor that binds to the allosteric site of kinases is BIRB 796. It binds to human p38

MAP kinase and stabilises the conformation of the kinase that is incompatible with ATP binding thus preventing ATP attachment to the active site (Pargellis *et al.,* 2002).

1.11 Objectives

PDK plays a significant role in glucose homeostasis through regulation of the PDC complex, and impaired functioning of PDC results in development metabolic disorders associated with abnormal glucose handling such as T2DM. Amongst the isomers of PDK, PDK4 is believed to be the primary isoform that is implicated in insulin resistance and T2DM. For that reason, it is important to find inhibitors of PDK4 for use in insulin-resistance or T2DM therapy.

To design inhibitors for PDK4, it is essential to understand its physical and chemical properties as well as its three dimensional structure. ADP was chosen as a lead candidate for this study, since it is known to bind to the PDK active site as a by-product of ATPase activity. Furthermore, ADP has been shown to inhibit PDK activity on its own as well as synergistically with pyruvate (Pratt and Roche, 1979). The PDK binding site of ADP has previously been mapped in rat PDK2 (Steussy *et al.,* 2001).

In order to study the physical properties of PDK4, the hypothetical structure of PDK4 was modelled on the resolved crystal structure of rat PDK2. The primary focus of the study was the ADP binding site since it enabled the investigation of the interactions between ADP and rat PDK4. Amino acid residues that were identified computationally to make contact with ADP were compared to those of rat PDK2 that are known to make contact with ADP. Further, the rPDK4 protein was expressed in *Escherichia coli* and

purified using affinity and gel filtration chromatography. The structure of PDK4 was then characterised using fluorescence spectroscopy and circular dichroism. The purified rPDK4 protein was further confirmed to be rPDK4 protein using Western blot analysis and a kinase activity assay. The binding of ADP and ATP to rPDK4 was studied using fluorescence quenching as both these ligands have been shown to quench the intrinsic tryptophan fluorescence of rPDK2 (Hiromasa *et al.,* 2006).

2 Materials and Methods

2.1 Materials

A plasmid containing the rPDK4 gene was a gift from Dr Kirill M. Popov of the University of Missouri-Kansas City (USA). Chromatographic resin used in this study (Sephacryl S-300HR and nickel-Sepharose), were purchased from Amersham Biosciences and Novagen®, respectively. The PDK4 primary antibody used in the Western blot analysis of rPDK4 was purchased from Roche Diagnostics. The rPDK4 substrate (Ac-YHGHSMSDPGVSYR) used in the PDK activity assay was synthesised by BIOPEP Peptide Synthesis at the Department of Biochemistry, University of Stellenbosch, South Africa. The radio-labeled ATP ([γ-^{32} P] ATP) used to determine rPDK4 activity was purchased from Amersham Pharmacia Biotech. All other reagents and chemicals used were of analytical grade.

2.2 Modelling of rPDK4

The protein sequences of rat PDK2 and PDK4 were aligned using ClustalW**,** version 1.83 (Thompson *et al.,* 1994**)**. Modelling of the structure of rPDK4 was exploited using the high sequence similarity between rPDK4 and rPDK2. The structure of rPDK4 was modelled based on the coordinates obtained from the tertiary structure of rat PDK2 (1JM6) by Steussy *et al*. (2001). The quality of the modelled structure was verified using the WHAT IF program (Vriend, 1990) and Ramachandran plot.

2.3 Identification of amino acid residues that are crucial for interacting with ADP

Since the rat PDK2 structure was co-crystallised with ADP, it was possible to study the putative ADP interaction with rPDK4. In order to investigate further the ADP interaction with rPDK4, the ADP from rPDK2 was merged to rPDK4 using DeepView/Swiss PDB (http://au.expasy.org/spdbv/) (Guex and Peitsch, 1997). The amino acids that play a role in hydrogen bonding interactions within a distance of 4 Å from ADP were investigated.

2.4 Confirmation of rPDK4 in pET28A plasmid

The rat cDNA was ligated into a pET28A vector and the resultant plasmid was transformed into *Escherichia coli* BL21 (DE3) cells that co-expressed the chaperones GroES/L. These proteins were expressed in a second plasmid (pGROELS, Takara, Japan). In order to confirm the presence of the rPDK4 gene, plasmid DNA was isolated a purified using the plasmid isolation kit from Promega as per the manufacturer's instructions. The isolated plasmid DNA was used as the template DNA in a polymerase chain reaction (PCR) using gene specific forward and reverse primers. The nucleotide sequences for the forward and reverse primers were the following: (5'-CCCTCCATGGTTGCACCATGAAGGC-3') and (5'-ACCCTCGAGAGCTGGGTCTA CATGGCC-3'). Each PCR reaction mixture contained 0.2 µM of each primer, 200 µM of deoxyribonucleic triphosphates, 10 ng of template DNA, buffer and 1 Unit of *Taq* polymerase. A forty cycle PCR reaction was performed with the following parameters: 45 seconds at 94ºC for denaturation, 1 minute at 60ºC for annealing and 1 minute at 72ºC for extension. The PCR product was cleaned using the PCR clean up kit from Promega

as per manufacture's instructions. The PCR product was then sent to Inqaba Biotech (South Africa) for sequencing.

2.5 Expression of rPDK4 protein

A glycerol stock of *Escherichia coli* BL21 [pET-PDK4 / pGROEL/S] (10 µl) was inoculated into Luria Broth medium (10 g/l yeast extract, 10 g/l tryptone and 5 g/l NaCl) containing 45 µg/ml kanamycin and 35 µg/ml chloramphenicol. The cells were allowed to grow at 37°C. After the A_{600} reached 0.7-0.8, the culture was transferred to room temperature and induced with 0.4 mM isopropyl-β-D-thiogalactopyranoside (IPTG). Incubation continued for another 20-24 h at room temperature. After 20-24 h of induction, cells were harvested by centrifugation at 50 000 x g for 20 min, and subsequently the pellet was stored at -20°C until they were used.

In order to test for expression of PDK, the harvested cells were resuspended in 10 ml of binding buffer (40 mM imidazole, 4 M NaCl, 160 mM Tris-HCl pH, 7.9) which was supplemented with 0.5 % (w/v) Triton X-100. The resuspended cells were sonicated and centrifuged at 50 000 x g for 30 min at 4 °C. The cleared cell lysate was analysed using sodium dodecyl sulphate polyacrylamide gel electrophoresis (SDS-PAGE) for rPDK4 expression (see section 2.7).

2.6 Purification of rPDK4 protein

The rPDK4 protein was purified using affinity and gel filtration chromatography.

2.6.1 Affinity chromatography

The cleared cell lysate was loaded onto a nickel-Sepharose column (7.5 ml bed volume) pre-equilibrated with the previously described binding buffer (see section 2.5). Once all the supernatant entered the resin, the column was washed with 5 volumes of binding buffer. The unbound protein was eluted with washing buffer (480 mM imidazole, 4 M NaCl, 160 mM Tris-HCl, pH 7.9) and the fractions were being monitored at 280 nm. The bound proteins were eluted with elution buffer (4 M imidazole, 2 M NaCl, 80 mM Tris-HCl, pH 7.9). The elution profile of the eluant was recorded by collecting 2 ml fractions and measuring the absorbance at 280 nm. Eluted fractions were analysed using SDS-PAGE (Section 2.7). The fractions that contained PDK were pooled and desalted on a PD-10 column (Pharmacia) equilibrated with storage buffer (20 mM Tris-HCl, 0.1 M NaCl, 0.5 mM EDTA, 0.05 % Triton X-100, 5 mM dithiothreitol (DTT), pH 8.0).

2.6.2 Gel filtration chromatography

Sephacryl S-300HR gel filtration media (Amersham Biosciences) with a fractionation range in relative molecular mass (M_r) of 1 x 10^4 - 1.5 × 10^6 was used for gel filtration chromatography. After packing the Sephacryl S300HR resin into the column, it was equilibrated with storage buffer (as described in Section 2.6.1). Gel filtration standards (Bio-Rad) with M_r of 670 000 (bovine thyroglobulin), 158 000 (bovine gamma globulin), 44 000 (chicken ovalbumin), 17 000 (horse myoglobin) and 1 350 (vitamin B-12) were used to create a size-exclusion standard curve. The gel filtration selectivity curve was created for the column according to the protocol laid out in the Gel Filtration Principles and Methods Handbook by Amersham Biosciences (Uppsala, Sweden). Blue dextrin (M_r

$2x10^5$) was used to determine the void volume (V_o) of the column. The partially purified PDK sample from the affinity purification column was loaded onto the column using a flow rate of 0.5 ml/min and the elution was monitored at $A_{280.}$ The eluted fractions that contained protein were analysed using SDS-PAGE.

The fractions that contained pure PDK protein were pooled and concentrated using Amicon ultra filtration unit. The final preparation was made to 50 % (v/v) with glycerol and stored in 50 µl aliquots at -80°C.

2.7 Sodium Dodecyl Sulphate Polyacrylamide Gel Electrophoresis (SDS-PAGE)

The purity and homogeneity of the rPDK4 protein were assessed using 10 % SDS-PAGE as described by Laemmli (1970). Prior to loading of protein samples onto the gel, the proteins were incubated with SDS-PAGE sample buffer (0.125 M Tris-HCl, 4 % (w/v) SDS, 20 % (v/v) glycerol, 5 % (v/v) β-mercaptoethanol and 0.02 % (w/v) bromophenol blue, pH 6.8) for 5 minutes at 95°C. Gels were electrophorised for one hour at 200 V. Staining was performed using Coomassie Stain (40 % methanol; 0.7 % acetic acid; 0.075 % Coomassie dye). Gels were destained with Coomassie destain (40 % methanol; 0.7 % acetic acid). Molecular weight markers (Fermentas) were used as standards with relative molecular masses of 250 000, 150 000, 100 000, 75 000, 50 000, 37 000, 25 000, 15 000 and 10 000.

2.8 Protein concentration determination

2.8.1 Beer-Lambert law

The protein concentrations were determined spectrophotometrically by applying the Beer-Lambert law.

The Beer-Lamberts law: $A = \varepsilon_\lambda cl$ (1)

where ε_λ is the molar extinction coefficient at wavelength λ, *c* is the concentration and *l* is the pathlength of the light through the solution in the cuvette. The extinction coefficient of the dimeric form of PDK was calculated using equation 2. The primary amino acid sequence of rPDK4 (Figure 5) was used to obtain the number of tryptophan, tyrosine and cysteine residues.

$$\varepsilon(280)(M^{-1}\,cm^{-1}) = (\#Trp)(5550) + (\#Tyr)(1340) + (\#Cys)(150) \quad (2)$$

$$= 2200 + 21440 + 1500$$

$$= 25140$$

2.9 Western blot analysis

The transfer of proteins from SDS-PAGE to polyvinylidene difluoride membranes (0.45 µm pore size, Immobilon-P, Millipore Corp., Bedford, MA) was accomplished with a semi dry Trans-Blot transfer system (Bio-Rad Laboratories, Inc.) with a transfer buffer

consisting of 25 mM Tris-HCl, 192 mM glycine, and 20 % methanol for one hour at 150 mA. Membranes were blocked for 90 min at room temperature in Tris buffered saline (TBS) containing Tween 20 (20 mM Tris (pH 7.6), 137 mM sodium chloride, 0.1 % Tween-20 (TBST)) and 2 % dried non-fat milk powder. Membranes were incubated overnight in TBST at 4 ºC with anti-PDK4 primary antibody at a dilution of 1:5000. After incubation with primary antibody, blots were incubated with antirabbit IgG horseradish peroxidase-conjugated antibodies at a dilution of 1:2500 in TBST for 90 min at room temperature. After three washes in TBST, immunoreactive bands were detected using the enhanced chemiluminescence detection system (Amersham Pharmacia Biotech, Arlington, IL), according to the manufacturer's instructions.

2.10 Size-exclusion high pressure liquid chromatography

Size-exclusion chromatography was performed on the partially purified PDK sample. The column used was TSK –Gel ® G2000SWXL. The column was equilibrated with 50 mM Na_2PO_4 pH 6.8. The buffer was filtered and degassed before use. An LKB 2150 pump (Pharmacia) was used to maintain the flow rate at 0.5 ml/min. Gel filtration standards (Bio-Rad) with relative molecular masses of 670 000 (bovine thyroglobulin), 158 000 (bovine gamma globulin), 44 000 (chicken ovalbumin), 17 000 (horse myoglobin) and 1 350 (vitamin B-12) were used to create a size-exclusion standard curve. The partially purified sample was then loaded and injected onto the column via the load/inject port, with the elution profile recorded at 280 nm using a Spectra series UV 100 detector. The protein was eluted with 50 mM Na_2PO_4 (pH 6.8) from the column at 0.5ml/min and the eluant was monitored at 280 nm.

2.11 PDK activity assay

The rPDK4 activity was determined using a modified published method (Jackson *et al.,* 1998). Briefly, the activity of rPDK4 was tested in a 30 µl reaction which contained 5µM of rPDK4, 25 µM of E1α peptide of PDC as a substrate (Ac-YHGHSMSDPGVSYR), [γ-^{32} P] ATP and activity assay buffer. The activity assay buffer contained the following: 44 mM Mops, 22 mM KH_2PO_4, 0.56 mM EDTA, 2 mM $MgCl_2$, 33 mM KCl and 2.2 mM DTT (pH 7.5) . The reaction was started with the addition of 2.5 µl of 250 µCi of [γ-^{32}P] ATP. This was followed by incubating the assay reaction at 37^{o}C for one hour. The reaction was terminated by addition of 10 µl of SDS-PAGE sample buffer and further incubating the sample at 90 ^{o}C for five minutes. The sample was loaded on 10 % SDS-PAGE gel and electrophorised as described in section 2.7. This was followed by staining the 10 % SDS-PAGE with Coomassie Stain and destaining overnight with Coomassie destain containing 10 % of glycerol. The gel was subsequently dried under vacuum and exposed on X-ray film at -70 ^{o}C overnight.

The activity of PDK is inhibited by ADP and pyruvate (Pratt and Roche, 1979). ADP and pyruvate were therefore also added to the kinase assay reaction in order to investigate their ability to inhibit the activity of rPDK4. The final concentration of ADP and pyruvate in the PDK activity assay were 50 mM each. The inhibition of rPDK4 activity would be shown by the inability of rPDK4 to phosphorylate the E1α peptide of PDC.

2.12 Circular dichroism

The far–UV CD spectrum of rPDK4 protein was measured 20^{o}C at using a Jasco J-810 spectropolarimeter. The sample chamber was constantly flushed with nitrogen. Far-UV CD spectra were recorded from 200 to 250 nm in a 0.2 cm quartz curvette at 1 nm intervals using a protein concentration of 2 μM in 20 mM sodium phosphate buffer, pH 7.5. The spectra were averaged over ten accumulations. The spectrum of the buffer control was subtracted from the experimental spectra.

2.13 Fluorescence spectroscopy

A fluorescence spectrum of PDK4 protein was obtained at 20 ^{o}C using a Perkin-Elmer LS 50 B spectrometer. The PDK4 protein was excited at either 280 nm or 295 nm. The excitation and emission bandwidths were set at 5 nm and the emission spectra collected at 200 nm/min with ten accumulations. The protein concentration used was 5 μM in 50mM potassium phosphate buffer, pH 7.5 containing 0.5 mM EDTA, 2.0 mM $MgCl_2$. The fluorescence values were corrected for the buffer as blank.

2.14 Effects of ADP and ATP binding on rPDK4 intrinsic fluorescence

The binding of ADP and ATP to rPDK4 was studied by measuring the quenching of tryptophan fluorescence (Hiromasa *et al.,* 2006). The rPDK4 protein at (5 μM in 50 mM potassium phosphate, 0.5 mM EDTA, 2.0 mM $MgCl_2$, pH 7.5), was titrated with either ADP or ATP in a concentration range of 0 to 250 μM, and the fluorescence was

measured. The protein was excited at 295 nm and the fluorescence emission was recorded at 350 nm.

In the data analysis, the fluorescence of rPDK4 in the absence of ligand is the maximum fluorescence (Fmax) at 350 nm (Figure 26). The addition of ligand (ADP or ATP) to rPDK4 quenches the fluorescence (F) of rPDK4 relative to the absence of ligand. The percentage of quenching by ligands was therefore, calculated according to equation 3.

$$\text{Percentage quenching} = 100^* \frac{(F_{max} - F)}{F_{max}} \qquad (3)$$

where, F_{max} is the maximum fluorescence of rPDK4 in the absence of the ligand and F is the fluorescence of rPDK4 in the presence of ADP or ATP.

Sigma plot V8.0 (Jandel Corporation) was used to determine the dissociation constant (K_d) of ADP or ATP, the data was fitted on hyperbolic (Figure 28B and Figure 29B) curve using equation 4.

$$F = \frac{Fmax\ [S]}{K_m + [S]} \qquad (4)$$

where, K_m is the Michaelis constant in mM (K_m=K_d) giving the K_d value and S is the concentration of the ligand (ATP or ADP).

The data was further plotted on a Hill plot using (Log (F/F_{max} - F) against log [S]) to determine the Hill constant (n_H).

3 Results

3.1 Homology modelling of rPDK4

To find an appropriate template to model the structure of rPDK4, a BLAST (http://www.expasy.org/tools/blast; Altschul *et al.*, 1997) search using the primary sequence of rPDK4 was performed against the structural Protein Database (PDB). The results from the search are shown in Table 1 with 1JM6 (rat PDK2 PDB code) giving the best E value. The closer the E value is to zero, the better the chance of a correlation between the peptide sequences of any two proteins compared. This, therefore, means they are likely to be structurally and functionally related.

Table 1: Results of a BLAST search for sequence homologues to rPDK4 that have a known tertiary structure

PDB number	**Description**	**Resolution Å**	**E- value**
1jm6	Pyruvate dehydrogenase kinase Isozyme 2 containing ADP	2.50	e^{-135}
1gkz	Branched–chained α–ketoacid dehydrogenase complexed with ADP	2.2	$2e^{-38}$
1gjv	Branched–chained α–ketoacid dehydrogenase complexed with ATP-gamma	2.7	$2e^{-37}$
1gkx	Branched–chained α–ketoacid dehydrogenase complexed with ADP	2.3	$2e^{-47}$

The primary amino acid sequences of rPDK2 and rPDK4 were also aligned using the alignment program ClustalW (http://www.ebi.ac.uk/Tools/clustalw/). The alignment results showed 65 % sequence similarity between the two proteins (Figure 10). Successful modelling requires at least one experimentally solved three-dimensional structure that should have more than 40 % amino acid sequence identity to the target sequence (Brenner, 2001 and Schwede *et al.,* 2003). Therefore, the BLAST search and sequence alignment result shows that the rPDK2 structure, 1JM6, is a suitable template for modelling rPDK4.

The modelled structure of rPDK4 was built using rPDK2 as a template using SWISS-MODEL (Guex and Peitsch, 1997). The proposed homology model of rPDK4 is shown in Figure 11. The quality of the modelled structure of rPDK4 was verified using the WHATIF program (Vriend, 1990) and the Ramachandran plot (Ramachandran and Sasiskharan, 1968). The Z scores of rPDK4 structure obtained from the WHATIF program was within the accepted range. The Ramachandran plot indicated that the modelled rPDK4 structure has good geometry (Figure 12). Most of the non-glycine residues were found in the favoured and allowed regions, with the exception of Ala^{33}, Pro^{134} and Ala^{313}. Although, some glycine residues were also found in the disallowed regions, this is acceptable since glycine has a hydrogen atom as a side chain which enables it to adopt a number of different conformations.

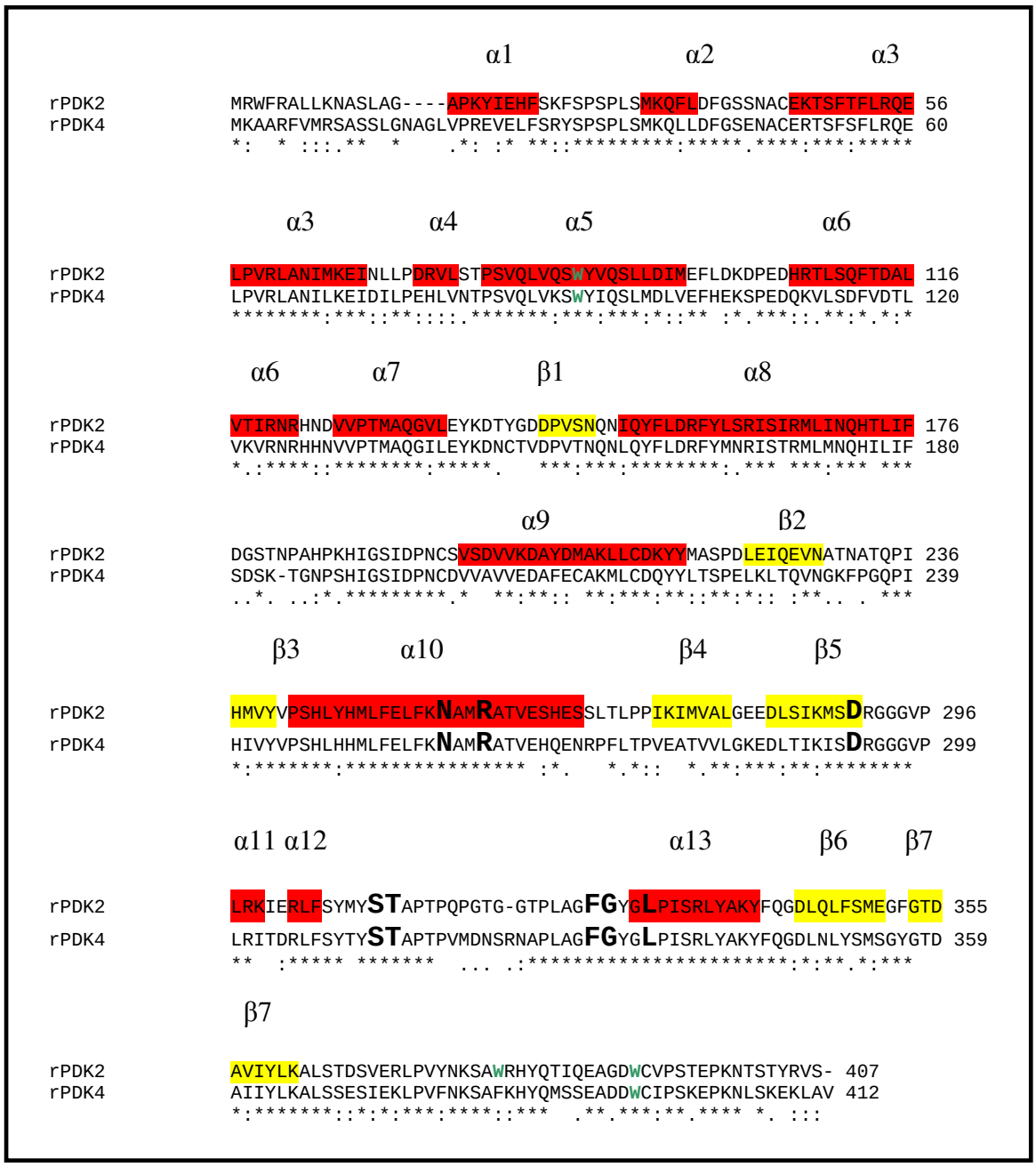

Figure 10: Alignment of rPDK2 and rPDK4.

The sequence was aligned using ClustalW, version 1.83 (Thompson *et al.,* 1994). The sequences of the PDK isomers were obtained from Genbank and their accession numbers are as follows: rPDK2-Q64536 and rPDK4-O54937. The red and yellow colours indicate α helices and β strands, respectively. The amino acids that are shown in bigger font, and in bold, are involved in the binding of ADP by PDK protein. The tryptophan residues (W) are shown in green. The secondary structure information was taken from http://www.biochem.ucl.ac.uk/bsm/pdbsum/1jm6. The similarity between the two sequences was determined using the NCBI BLASTP 2.2.8 (Altschul *et al.*, 1997).

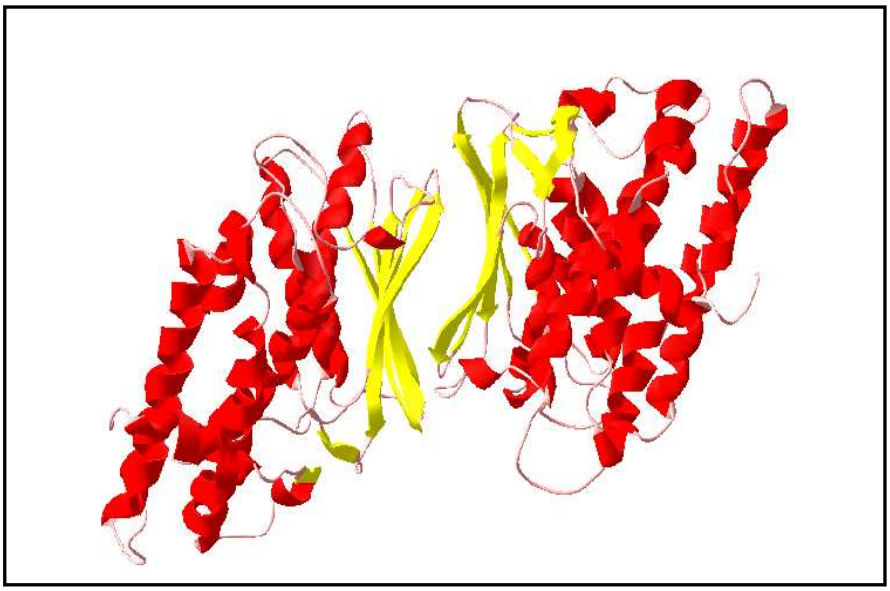

Figure 11: Ribbon representation of the homology modelled three dimension structure of rat PDK4.

Ribbon presentation of human PDK4 dimer modelled using SWISS-MODEL based on coordinates published by Steussy *et al*. (2001) (1JM6) viewed down the 2-fold axis. α-Helices are coloured in red, β-strands are coloured in yellow, and the loop regions are coloured in pink.

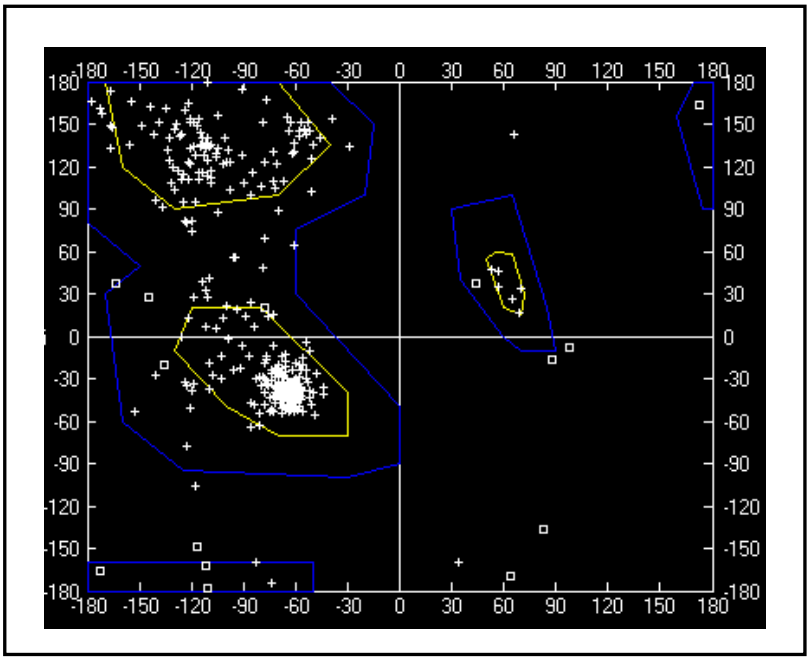

Figure 12: Ramachandran plot of rat PDK4 structure.

Yellow lines indicate favoured conformations of amino acid residues, and blue lines indicate additional allowed conformations. Points that are boxes indicate glycine residues and crosses indicate other residues.

The overall structural topology of rPDK2 seems to be preserved in rPDK4 according to the SWISS-MODEL homology modelling. The structural alignments between these two structures give a root mean square deviation (RMSD) value of 1.7 Å using the backbone of all atoms of both structures (Figure 13). The RMSD value is used to measure the structural similarity between proteins structures (Maiti *et al*., 2004). This RMSD value of 1.7 Å obtained from aligning the rPDK4 model and its template, implies that the overall structural topology is highly conserved and does not deviate far from the crystal structure of PDK2. In the structural alignment, the modelled rPDK4 is coloured using the confidence factor which indicates regions that have deviated from the template. The regions that have deviated significantly are in coloured red. The modelled structure of rPDK4 is relatively good since most of the structure is coloured green (Figure 13) indicating no deviation from the template structure. However, there are regions of rPDK4 that are coloured red. These regions are (a) amino acid residues Phe^{28}- Glu^{31} which form a loop connecting helices α2 and α3, (b) amino acid residues Glu^{125}- Pro^{134} which form a loop region connecting helix α7 and β1 strand, (c) residues Phe^{165}- Pro^{173} which are part of a loop region connecting helices α8 and α9 and (d) residues Asp^{305}- Lue^{312} which are part of the loop region connecting helices α12 and α13. The above regions are coloured red because they were constructed *ab initio* since they are missing in the crystal structure of rPDK2 and this lowers the level of confidence in the integrity of constructed region of the rPDK4 modelled structure.

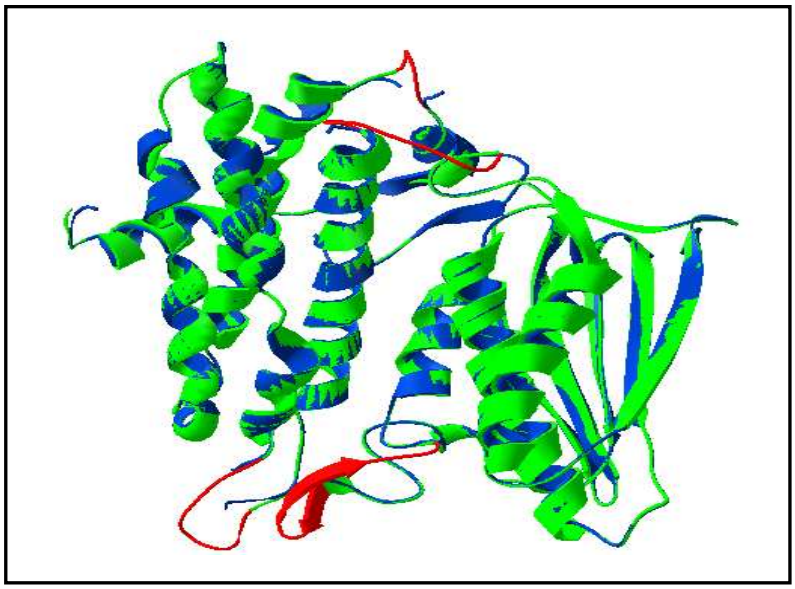

Figure 13: Structural alignment of rat PDK2 and rat PDK4 monomers.

Rat PDK4 is coloured by confidence factor (green and red) where the coloured red shows the regions that were constructed *ab initio*. The rat PDK2 is coloured blue.

3.2 The rPDK4 nucleotide binding site

The ADP binding site in rPDK4 was located by identifying the presence of binding pockets on the protein surface. Figure 14 shows two cavities indicated in red and blue colouring on the rPDK4 protein surface which is coloured yellow. The red coloured cavity was determined to be 261 Å and this site has not yet been characterised. The blue coloured cavity has a surface area of 94 Å which correspond to the size of ADP binding pocket in rPDK2. The manual docking of ADP to rPDK4 also confirmed the 94 Å cavity as the ADP binding pocket. The ADP binding pocket consists of β-strand-loop-α-helix structure with the loop region being glycine rich. This structure is a characteristic feature of the phosphate binding site (Schulz *et al.*, 1986).

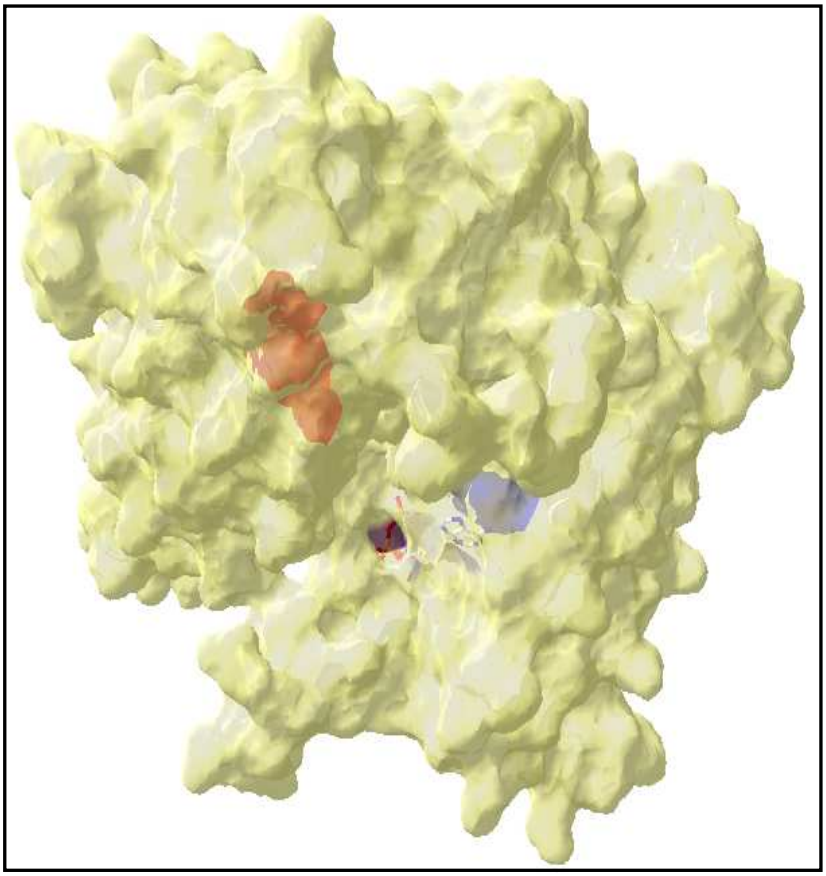

Figure 14: Molecular surface of rPDK4 showing the ADP binding site.

The image was generated using Swiss PDB Viewer (Guex and Peitsch, 1997). The molecular surface of rPDK4 is coloured yellow. The blue shaded region in the rPDK4 surface is the ADP binding site which contains an ADP molecule coloured according to CPK colour scheme . The red coloured region is a potential ligand binding site that has not yet been characterised.

The amino acids in the ADP binding site that play a role in the interaction between ADP and rPDK4 through hydrogen bond formation, were identified using DeepView/Swiss PDB Viewer (Guex and Peitsch, 1997). Hydrogen bonds that were formed within a distance of 4 Å from ADP are shown by dotted green lines in Figure 15. The ADP binding site of rPDK4 is homologous to that of rPDK2. Further, the amino acids that are involved in the binding of the ADP molecule in rPDK4 are the same as those in rPDK2

(Figure 15). The positions of the residues that are involved in the binding of ADP are shown in Figure 10.

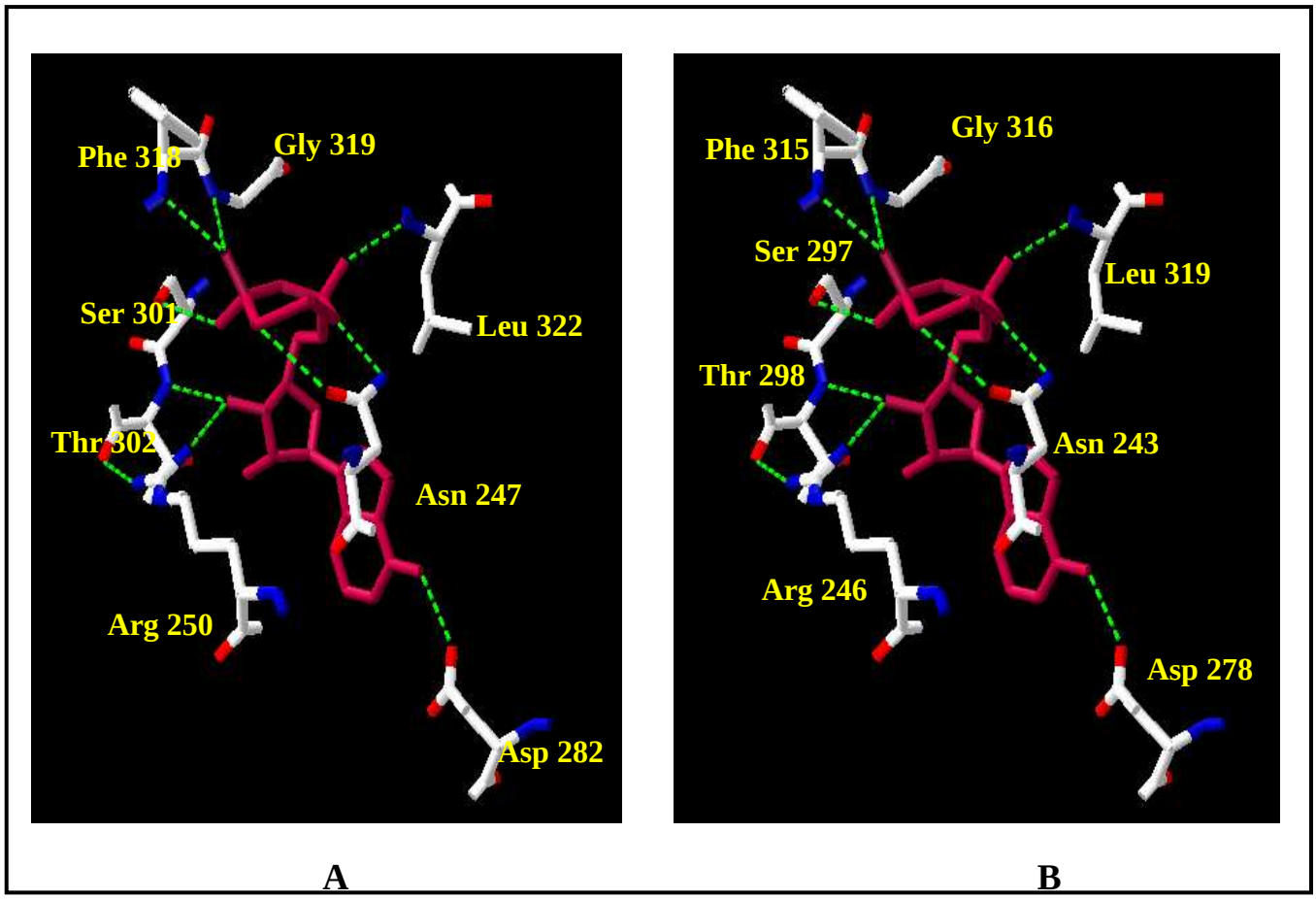

Figure 15: The interaction between rPDK4 and ADP and rPDK2 and ADP.

The image was generated using Swiss PDB Viewer (Guex and Peitsch, 1997). A: rat PDK2 interacting with ADP. B: rat PDK4 interacting with ADP. PDK is coloured in CPK colour scheme and ADP is coloured in pink. Hydrogen bonds between PDK and ADP are shown in dotted green lines. The participating residues are labelled using yellow font.

The ionic and hydrophobic interactions between ADP and rat PDK2 active site were investigated using Swiss PDB Viewer. The results are shown in Figure 16. In the rPDK4 ADP binding site, Arg^{246} and Asp^{278} were the two only residues that formed ionic

interactions with ADP. The rest of the amino acids were either involved in hydrophobic or hydrogen bonds.

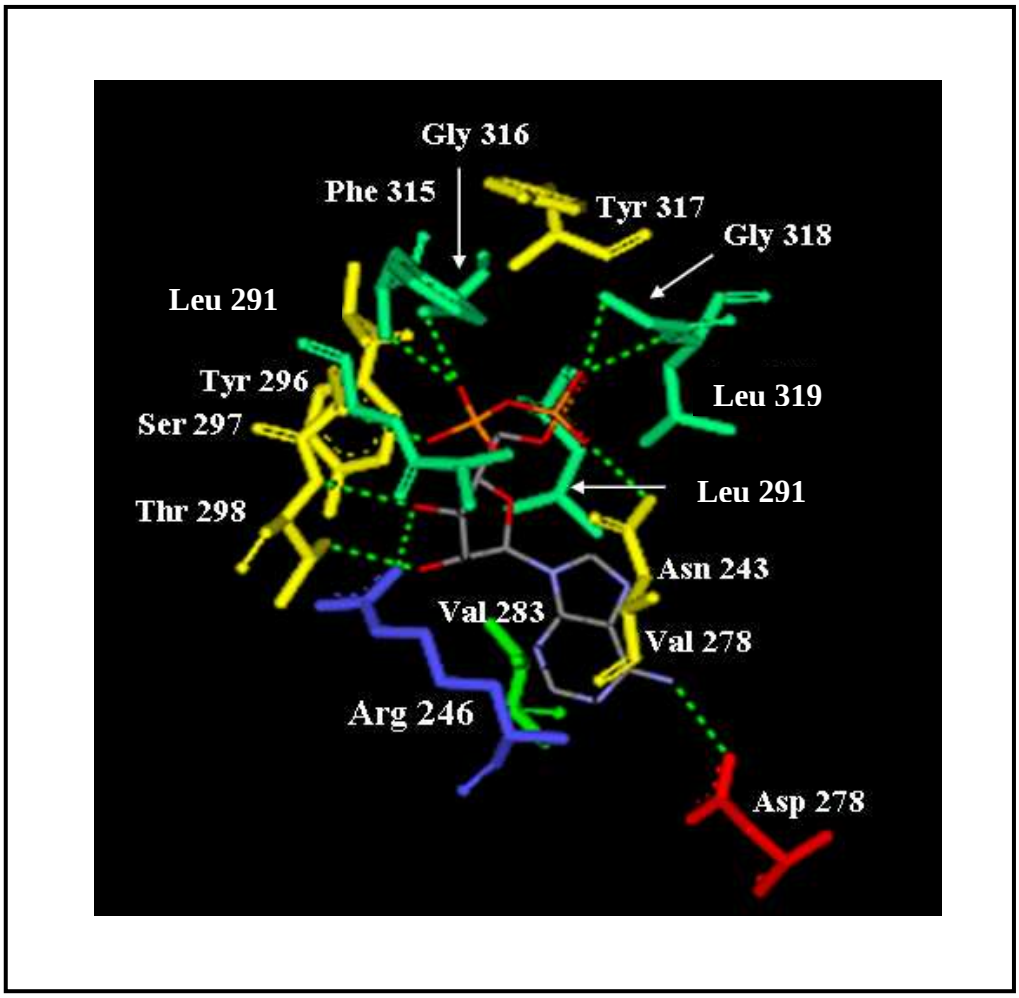

Figure 16: Non-covalent interactions between ADP and the residues in the nucleotide binding domain of rPDK4.

The ADP molecule is coloured according to CPK where red indicates region with negative charge. The dotted green lines indicate hydrogen bonds between ADP and residues of rPDK4. The residues of rPDK4 are coloured according to their properties with red: acidic, blue: basic, yellow: polar and green: non polar.

3.3 Purification and characterisation of rPDK4

3.3.1 Confirmation of rPDK4 in pET28A plasmid

The pET28/rPDK4 clone used in this study was a gift. It was, therefore, necessary to initially confirm whether it contained the rPDK4 gene. Plasmid DNA was isolated from five separate colonies of *Escherichia coli* BL21 [pET28/rPDK4] and used for the amplification of the PDK4 gene. As expected, a band of approximately 1.3 kb was obtained from all the colonies (Figure 17) and the 1.3 kb corresponds to the size of the PDK gene. The 1.3 kb PCR product was sequenced. The results from sequencing were submitted for a BLAST search (http://www.ncbi.nlm.nih.gov/BLAST) and gave a 100 % match to the nucleotide sequence of rPDK4.

3.3.2 Expression of rPDK4

PDK4 protein expression was induced as described in Section 2.5 using 0.4 mM of IPTG. Figure 18 shows the level of protein overproduction. High levels of protein expression were obtained between 16 to 24 hrs of induction (Figure 18, Lane 2 to Lane 4). The PDK4 protein was expressed and this was confirmed by the band at about 50 kDa. The predicted molecular mass of PDK4 is ~ 50 kDa. A band with low levels of induction was seen at 50 kDa, however a strongly induced band was seen at around 60 kDa. This protein was assumed to be GroEL (the bacterial heat shock protein 60 / Hsp60) since the PDK4 clone was transformed into *Escherichia coli* BL21 (DE3) cells that co-expressed

the chaperone GroEL with its co-chaperone GroES. They are the other proteins that were also induced during the expression of rPDK4 (Figure 18).

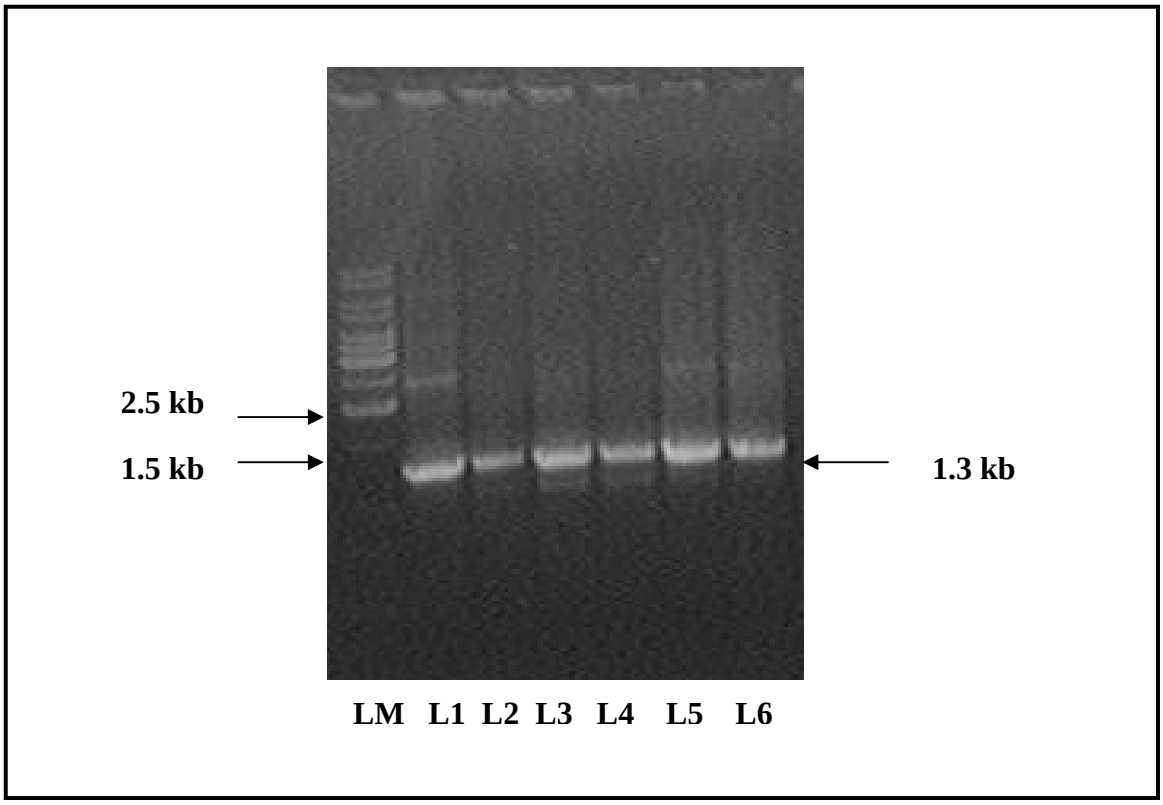

Figure 17: Amplification of the PDK4 gene from pET28/rPDK4 using gene specific forward and reverse primes.

Lane LM: contains the GeneRuler marker. Lanes 1 to 6: show the 1.3 kb gene of pET28/rPDK4. The molecular mass of the indicated bands are shown.

The expression of rPDK4 seemed low and it was therefore crucial to establish whether the rPDK4 protein was insoluble and thus located in the pellet. The cells that expressed high amounts of rPDK4 (induced for 24 hrs) were sonicated and centrifuged. Both the cleared cell lysate and pellet were analysed by SDS-PAGE for the presence of rPDK4. Figure 18, lane 6 shows that there was no significant amount of rPDK4 located in the pellet. Hence, rPDK4 was soluble.

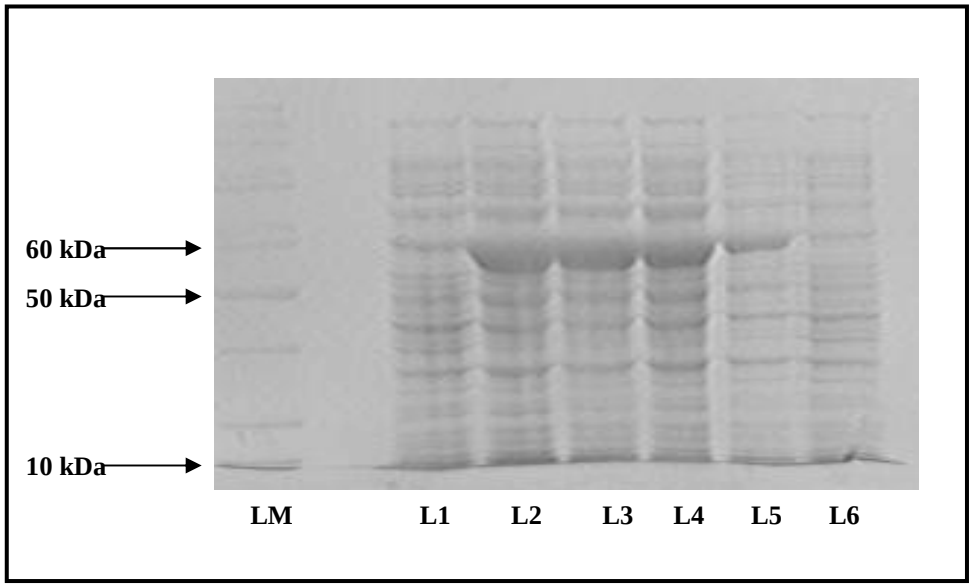

Figure 18: Expression of rPDK4 protein.

Lane M: Protein Ladder Marker; Lane1: contains un-induced (No IPTG) protein samples. Lanes: 2 to 5 show the induced protein samples. Samples were taken at 4 hourly intervals. Lane 2: 24 hrs; Lane 3: 20 hrs; Lane 4: 16 hrs; Lane 5: 12 hrs. Lane 6: contains insoluble proteins in the pellet after 24 hours of induction.

3.3.3 Affinity chromatography

After induction, the rPDK4 protein was purified using a nickel-Sepharose column under native conditions as outlined in the Material and Methods section 2.6.1. The purity and homogeneity of the rPDK4 was assessed using SDS-PAGE (Figure 19). Figure 19 lane 4 and lane 5 show proteins that did not bind to the nickel column while lane 2 and lane 3 show proteins that washed off during the washing steps. The proteins that eluted in the wash step included the highly expressed 60 kDa protein. During the wash steps there was, however a very small amount of PDK4 that was lost and this is confirmed by the band at about 50 kDa as seen in Figure 19 lanes 2 and 3. The rPDK4 protein was eluted

from the nickel column by using high concentrations of imidazole and sodium chloride. Figure 19 lane 1 shows that using nickel affinity column could only partially isolate PDK4 since there are still other proteins present.

3.3.4 Identification of rPDK4 by Western blotting

At this point, it was necessary to confirm whether the 50 kDa protein obtained through affinity chromatography was indeed rPDK4. It was decided to perform Western blot analysis on the partially purified protein from nickel affinity column using antibodies that are specific for rPDK4 protein. The protein that was thought to be rPDK4 gave a signal when treated with antibodies specific to rPDK4 protein (Figure 20). The signal was obtained at 50 kDa and this molecular weight corresponds to that of rPDK4.

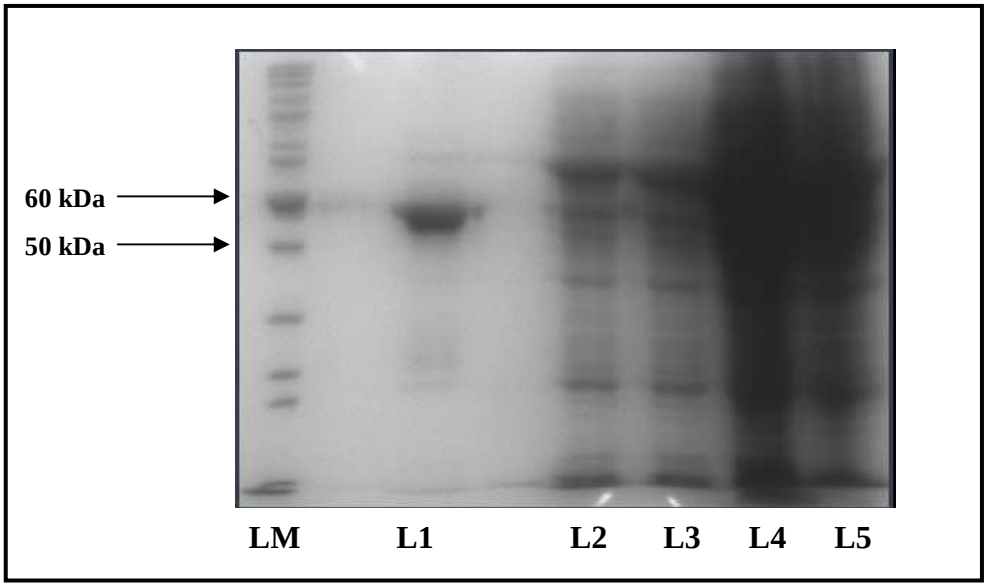

Figure 19: 10% SDS-PAGE gel showing purification of histidine tagged rPDK4 protein using nickel affinity chromatography.

Lane M: Protein Ladder Marker; Lane 1: contains the eluant from nickel affinity column; Lane 2: shows proteins that washed off with binding buffer; Lane 3: shows proteins that washed off with washing buffer. Lanes 4 and 5: contains proteins that did not bind to the column.

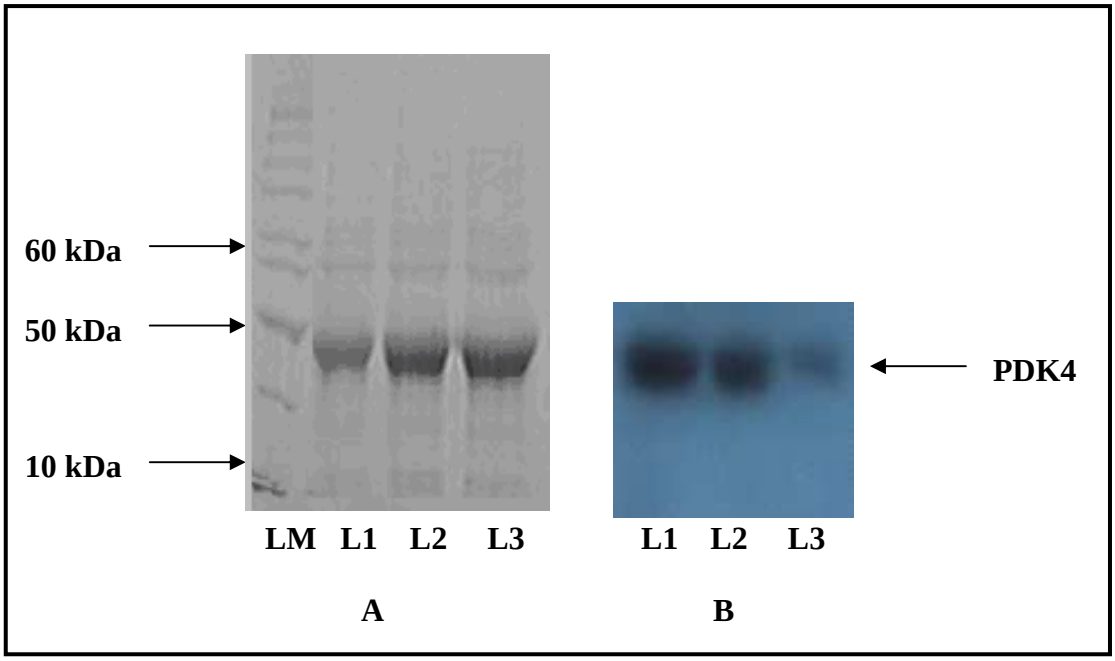

Figure 20: (A) 10% SDS-PAGE gel showing partially purified rPDK4 protein using nickel affinity chromatography, and (B) related Western blot analysis showing detection of rPDK4 protein.

Lane M: Protein Ladder Marker; Lane 1 to Lane 3: contains partially purified PDK4 protein with 100 µg, 150 µg and 200 µg of protein, respectively. Figure 20B: Western Blot detection of rPDK4 based on the samples on the SDS-PAGE gel Figure 20A.

3.3.5 Size-Exclusion chromatography

Purification of rPDK4 using nickel affinity chromatography did not result in pure rPDK4 protein. SDS-PAGE analysis showed that the rPDK4 protein was contaminated with other proteins (Figure 20A). It was, therefore, necessary to subject the partially purified enzyme to another purification step which was gel filtration. At present there is a vast selection of gel filtration methods with different exclusion limits. In order to select the

media that is most likely to give a good separation, the partially purified rPDK4 protein was analysed using SE-HPLC under native conditions.

A standard protein elution profile and corresponding standard curve were generated using molecular mass standards and a TSK –Gel ® G2000SW column. Native SE-HLPC confirmed that the rPDK4 purified through nickel affinity column was indeed contaminated with other proteins (Figure 21A). A protein with molecular mass of 96 kDa (retention time of 113 minutes) was obtained (Figure 21A). This molecular mass corresponds to the dimeric form of PDK (Steussy *et al.,* 2001 and Popov *et al.,* 1999). The molecular masses of other proteins contaminating the rPDK4 were found to be 279 and 139 kDa and these proteins are unlikely to be heat shock proteins. The standard curve of the elution profile for the protein standards is shown in Figure 21B. The molecular mass standard curve was used to estimate the mass of the proteins contained in the partially purified rPDK4 sample. Based on the SE-HPLC results, Sephacryl S-300HR gel filtration media (fractionation range of 1 x 10^4-1.5 × 10^6) was chosen to further purify rPDK4 from its contaminants.

A standard protein elution profile and corresponding standard curve were generated using molecular mass standards and Sephacryl S-300HR column. The proteins eluting from Sephacryl S-300HR column are shown in Figure 22 and a protein peak with the retention time of 116 minutes was observed. The molecular mass of this peak was estimated to be 97 kDa which corresponds to the dimeric form of PDK protein. Fractions 28 to 38, giving a total volume of 10 ml, were pooled and concentrated to 500 µl using Vivaspin 20 with a 30 kDa membrane cut-off. This protein sample was further confirmed to be rPDK4 using SDS-PAGE gel and Western blot analysis (Figure 23).

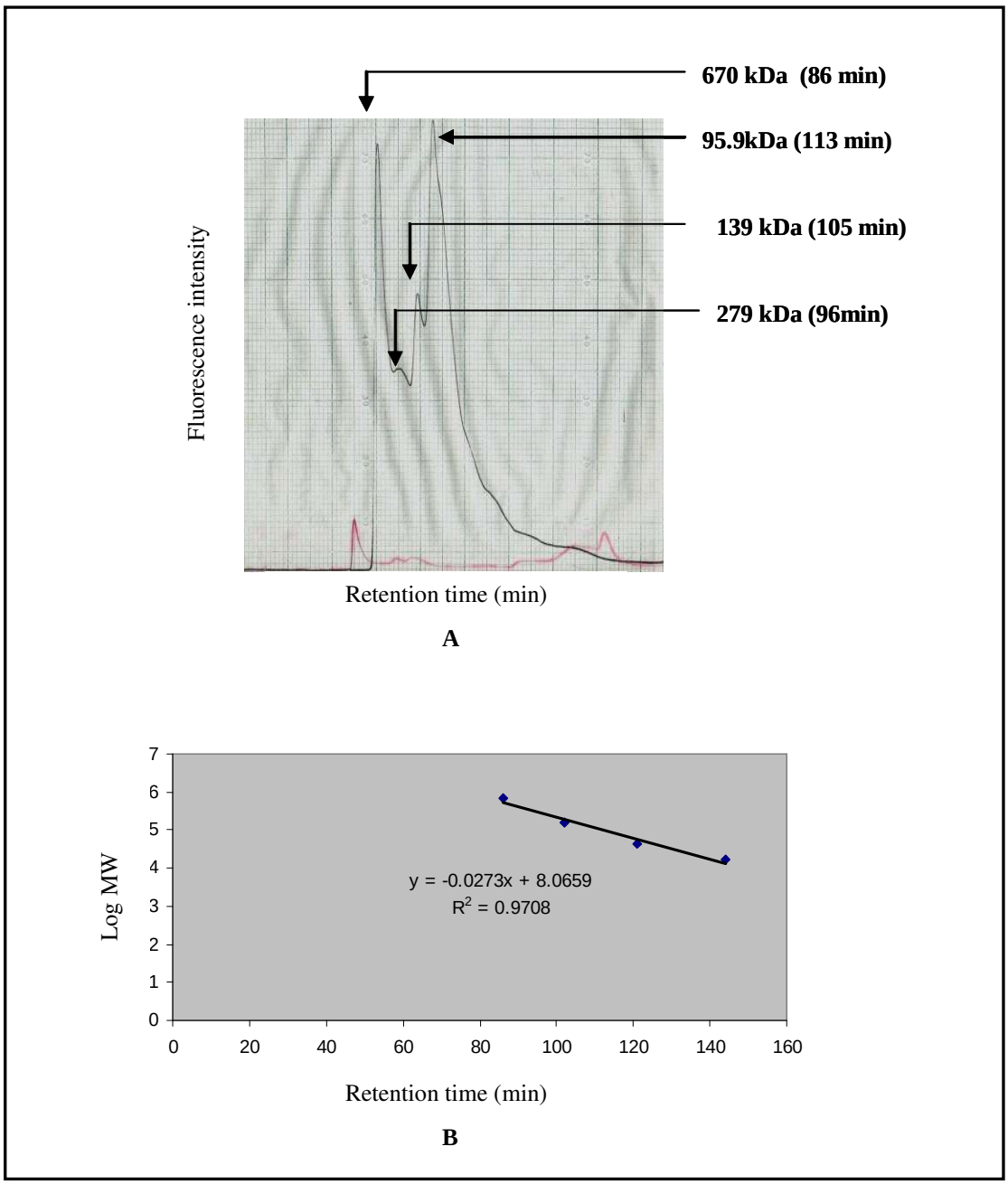

Figure 21: SE-HPLC elution profile of partially purified rPDK4.

The elution profile of partially purified rPDK4 protein using a TSK–Gel ® G2000SW column. Briefly, the partially purified rPDK4 protein was injected into the SE-HPLC column and the effluent was monitored at 280 nm. The retention times are shown in brackets next to the protein peaks. The relative molecular masses of the proteins that eluted from the SE-HPLC column were estimated using the standard curve in Figure 21B.

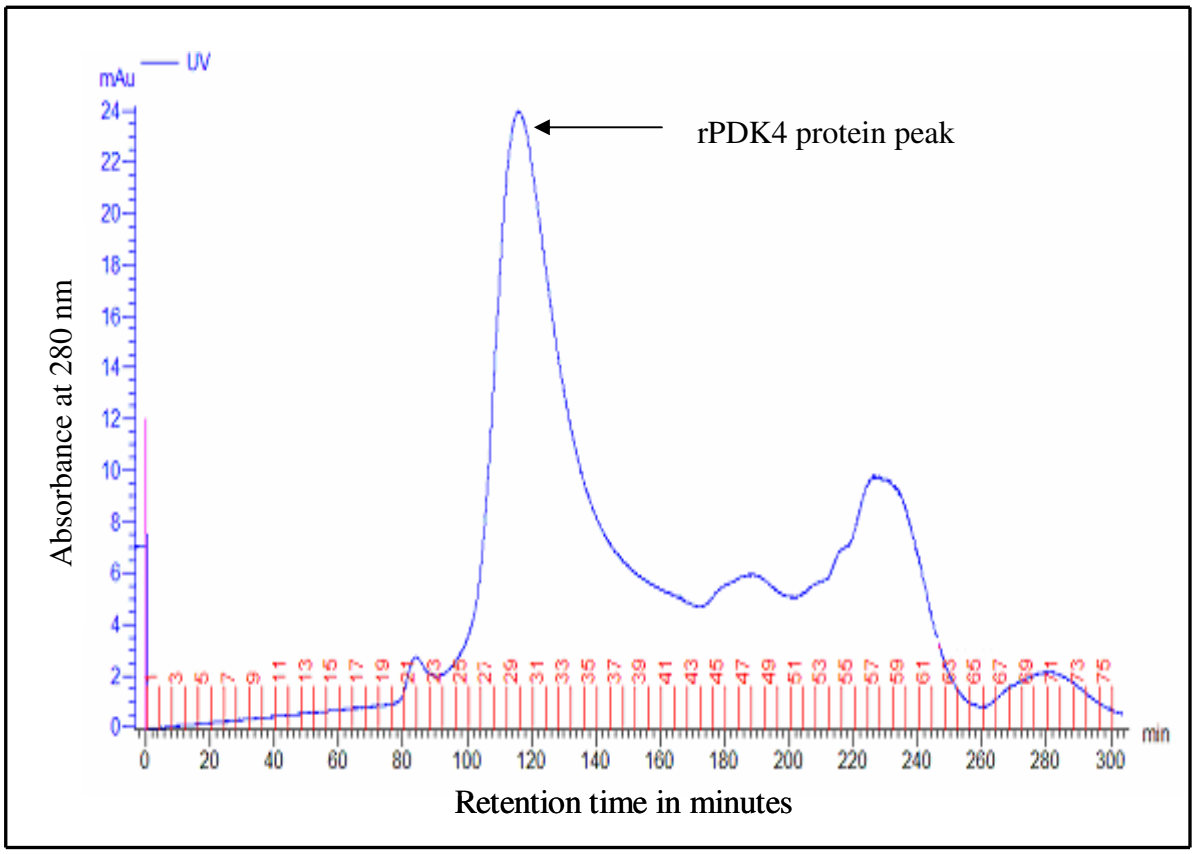

Figure 22: Protein elution profile from Sephacryl S-300HR of partially purified rPDK4.

The partially purified rPDK4 from the affinity chromatography step was concentrated 10 fold using a 30 kDa cut-off membrane. A total volume of 2 ml of protein (6 mg) was loaded onto the Sephacryl S-300HR column and eluted using sodium phosphate buffer with a flow rate of 0.5 ml/min. The elution of the protein was monitored at 280 nm.

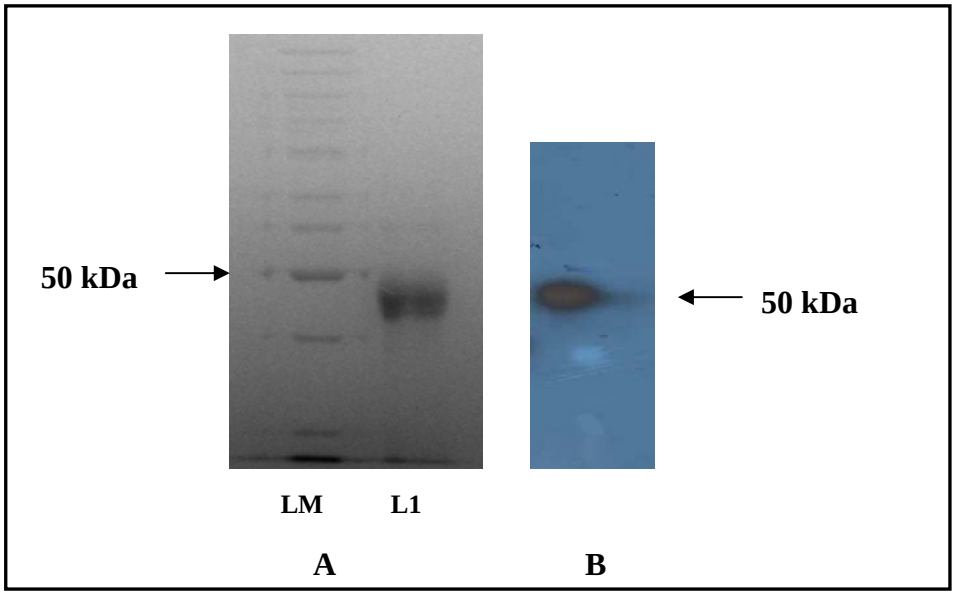

Figure 23: Purification of rPDK4 protein by gel filtration.

The 10 % SDS-PAGE gel analysis of rPDK4 from gel filtration is depicted in A. Lane LM: shows the protein ladder marker, and L1 contains the eluant from gel filtration with retention time of 116 minutes. The Western blot analysis of protein sample on the SDS-PAGE gel is shown in B.

3.3.6 Activity of rPDK4

It was of importance to determine whether the isolated rPDK4 protein was catalytically active. PDK proteins are known to phosphorylate three serine residues (Ser^{264}, Ser^{271}, Ser^{203}) in the E1α subunit of PDC (Sale and Randle, 1981). Jackson *et al*. (1998) demonstrated that rPDK2 protein can phosphorylate the peptide Ac–YHGHSMSDPGVSR since it resembles the protein sequence region of E1α that is phosphorylated by PDK proteins. The rPDK4 protein isolated in this study was found to be active since the data in Figure 24 demonstrates that the peptide was phosphorylated. PDK proteins are reported to undergo autophosphorylation (Popov *et al.,* 1993; Thelen *et al.,* 2000) and lane 2 in Figure 24 demonstrates this. The presence of ADP or pyruvate, or both, in the peptide phosphorylation assay inhibited rPDK4 autophosphorylation as

well as the phosphorylation of the peptide (Figure 24, Lanes 3 and 4). This is consistent with published data which reports ADP and pyruvate are amongst the inhibitors of PDK enzymes.

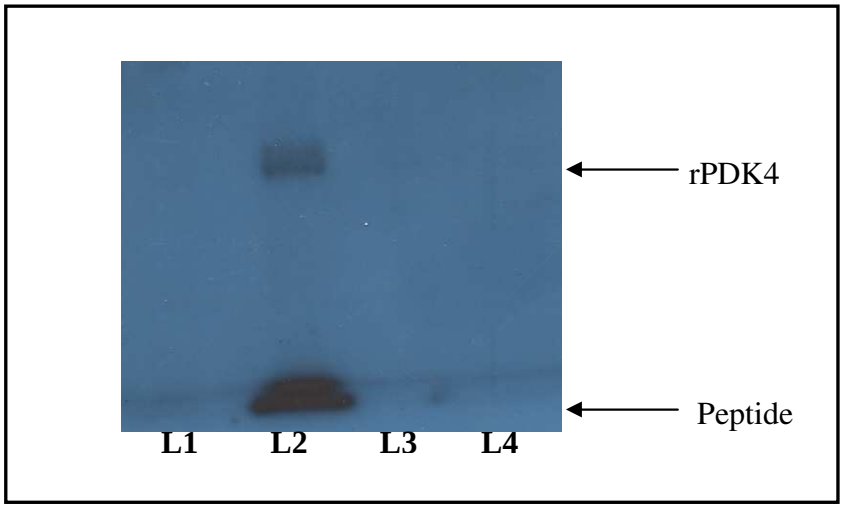

Figure 24: Autoradiograph showing the auto-phosphorylation of rPDK4 and peptide phosphorylation.

The peptide was phosphorylated as described in section 2.11. The proteins were separated by 10% SDS – PAGE gel. The auto-phosphorylated rPDK4 and the phosphorylated peptide were detected by autoradiography. L1: contains a negative control (no rPDK4 protein); L2: shows an auto-phosphorylated rPDK4 and phosphorylated peptide; L3 and L4: shows inhibition of rPDK4 auto-phosphorylation and phosphorylation of peptide by ADP and pyruvate respectively.

3.3.7 Circular dichroism (CD)

Far-UV CD was used to study the secondary structural content of the purified rPDK4 protein. The far–UV CD spectrum shows that rPDK4 displays two ellipticity minima at 208 and 222 nm (Figure 25). These wavelength minima are an indication of a protein with high helical content and which is consistent with the structure of PDK proteins that contain about 69 % α-helices (Steussy *et al.,* 2001 and Figure 11).

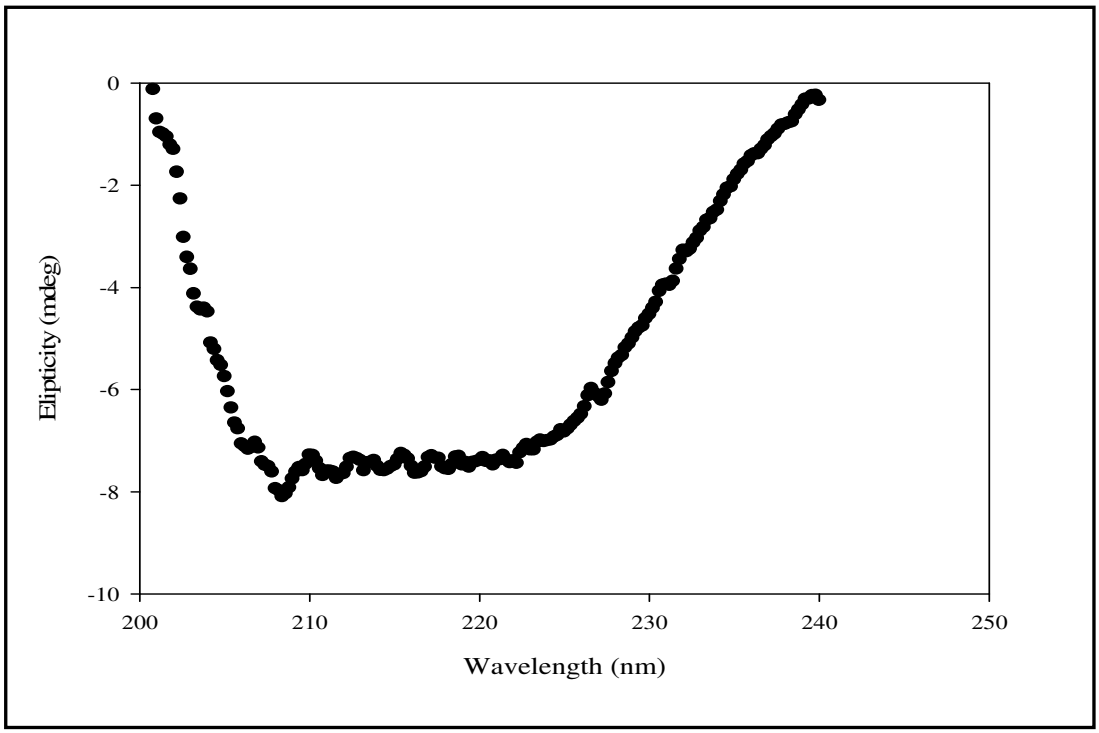

Figure 25: Far-UV CD spectra of rPDK4.

The rPDK4 protein (2 μM) in phosphate buffer was subjected to circular dichroism to determine its secondary structure content. The spectrum of the buffer control was subtracted from the experimental spectra.

3.3.8 Fluorescence spectroscopy

Amino acid sequence analysis of rPDK4 shows that it contains tyrosine and tryptophan residues (Figure 10). These amino acid residues fluoresce when excited at 280 nm. Fluorescence spectroscopy was therefore used to further characterize rPDK4. The basal fluorescence of rPDK4 was measured by exciting the rPDK4 at 280 nm where both the tyrosine and tryptophan are known to fluoresce. The rPDK4 protein was also excited at 295 nm exclusively for tryptophan residues. The excitation of PDK4 protein at 295 nm with emission wavelength between 300 and 420 nm showed a broad peak with a peak

centre of 350 nm whereas exciting the rPDK4 at 280 nm gave higher fluorescence intensity with peak centre of 318 nm (Figure 26).

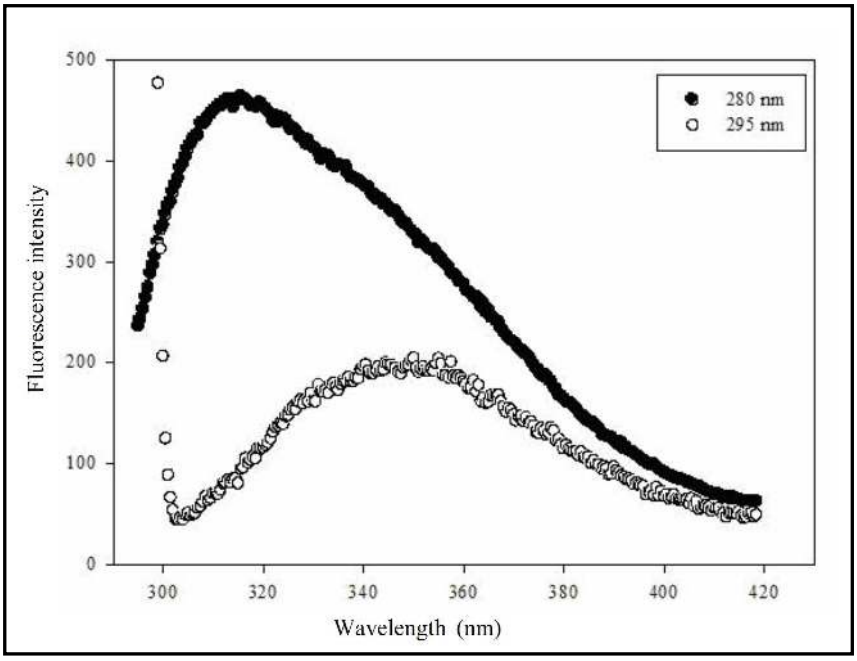

Figure 26: Basal fluorescence spectrum of 5 µM rPDK4 protein.

Briefly, 5 µM of rPDK4 protein was excited at 280 nm (black solid circles) and 295 nm (clear circles) and the emission wavelength was measured between 300 and 420 nm.

3.3.9 Effects of ADP and ATP binding on the rPDK4 intrinsic fluorescence

Hiromasa *et al.* (2006) reported that mutation of Trp^{383} on human PDK2 to phenylalanine results in the loss of basal fluorescence of human PDK2 when excited at 295 nm. This meant that Trp^{383} was the main tryptophan residue responsible for the fluorescence when human PDK2 is excited at 295 nm and the other two tryptophan residues on human PDK2 (Trp^{79} and Trp^{371}) were buried within the structure thus becoming solvent inaccessible (Hiromasa *et al.,* 2006; Figure 27).

In the tertiary structure of human PDK2, Trp^{383} is situated close to the binding site (Figure 27). The fluorescence emitted by Trp^{383} can therefore be used to monitor any effects of ligand binding (ADP or ATP) to the binding site. It would therefore be expected to see a change in the fluorescence emission when a ligand (ADP or ATP) binds in the PDK active site, since the presence of a ligand would affect the environment of Trp^{383}. In an event where there is no binding the fluorescence intensity is unlikely to change.

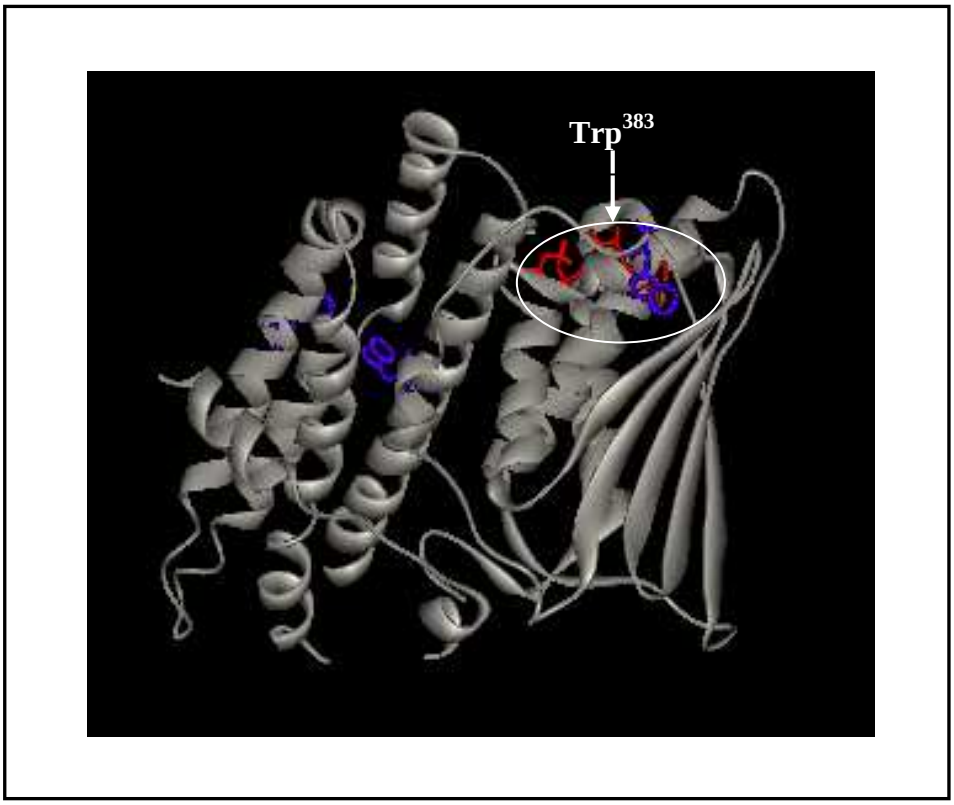

Figure 27: The structure of human PDK2 monomer (2bu2) complex with ATP showing the location of the tryptophan residues.

The tryptophan residues are shown in blue and the ADP molecule is coloured red. The region circled in white depicts the nucleotide binding site.

Primary sequence analysis of rPDK4 showed that it contained two tryptophan residues, Trp^{81} and Trp^{395}. The $Trp^{395}$of rPDK4 corresponds to Trp^{383} in human PDK2. It was

therefore hypothesised that Trp^{395} in rPDK4 could also be used to study binding of ADP and ATP. In the modelled structure, the Trp^{395} residue is in a loop region at the tail of the C-terminal domain, but, when the PDK4 is correctly folded it is located in close proximity to the active site (Figure 27). It was therefore hypothesized that Trp^{395} in rPDK4 will also be situated close to the active site in the tertiary structure of rPDK4 and hence might be sensitive to the binding of ADP and ATP.

It is shown in Figure 28A, that an increase in the concentration of ADP present in solution with rPDK4 results in a decrease in tryptophan fluorescence intensity putatively given by Trp^{383}. The dissociation constant (K_d) of ADP was determined to be 37 µM when the data was fitted on the hyperbolic fit using equation 4 (Figure 28B). Steussy *et al* (2001) reported that each monomer of PDK contains an ADP binding site. It was, therefore, necessary to establish further whether there was any cooperativity between the two ADP binding sites of rPDK4. The data was further analysed using a Hill plot (Figure 28C). The Hill plot gave a Hill coefficient (n_H) value of 0.7 which is indicative of negative cooperativity within the two ADP binding site of rPDK4. The n_H of 0.7 differs with the value of 1 published by Hiromasa *et al*. (2006) which described positive cooperativity within the two human PDK2 binding sites of ADP.

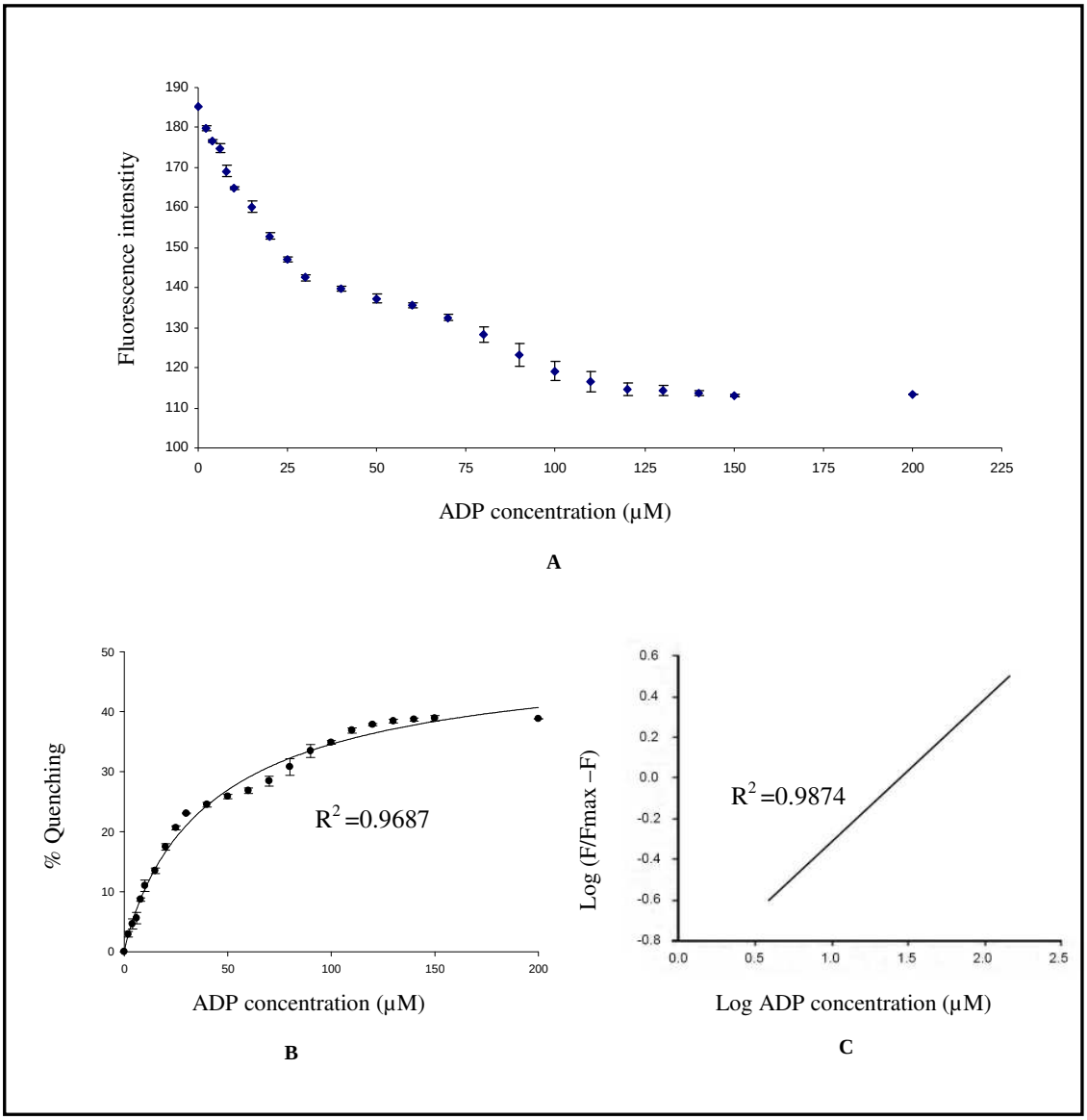

Figure 28: Quenching of basal rPDK4 fluorescence at 350 nm by ADP.

The rPDK4 (5 µM) was excited at 295 nm and the fluorescence was measured at 350 nm.

The ATP molecule also binds rPDK4 at the same site as ADP and it was of interest to determine whether the binding of ATP to rPDK4 has similar effects on the basal fluorescence of this protein as ADP. Figure 29A depicts a reduction in fluorescence of rPDK4 with increasing amounts of ATP. The maximum quenching effect for ATP on Trp^{383} fluorescence was 31 % (Figure 29B) and this was similar to 38 % for ADP (Figure 28B). The percentage quenching values obtained in this current work (calculated using equation 3) were below those reported by Hiromasa and co workers (2006) which were

53 % for ATP and 48 % for ADP. The K_d value for ATP was determined to be 17.4 µM when the data was fitted on the hyperbolic fit (Figure 29C).

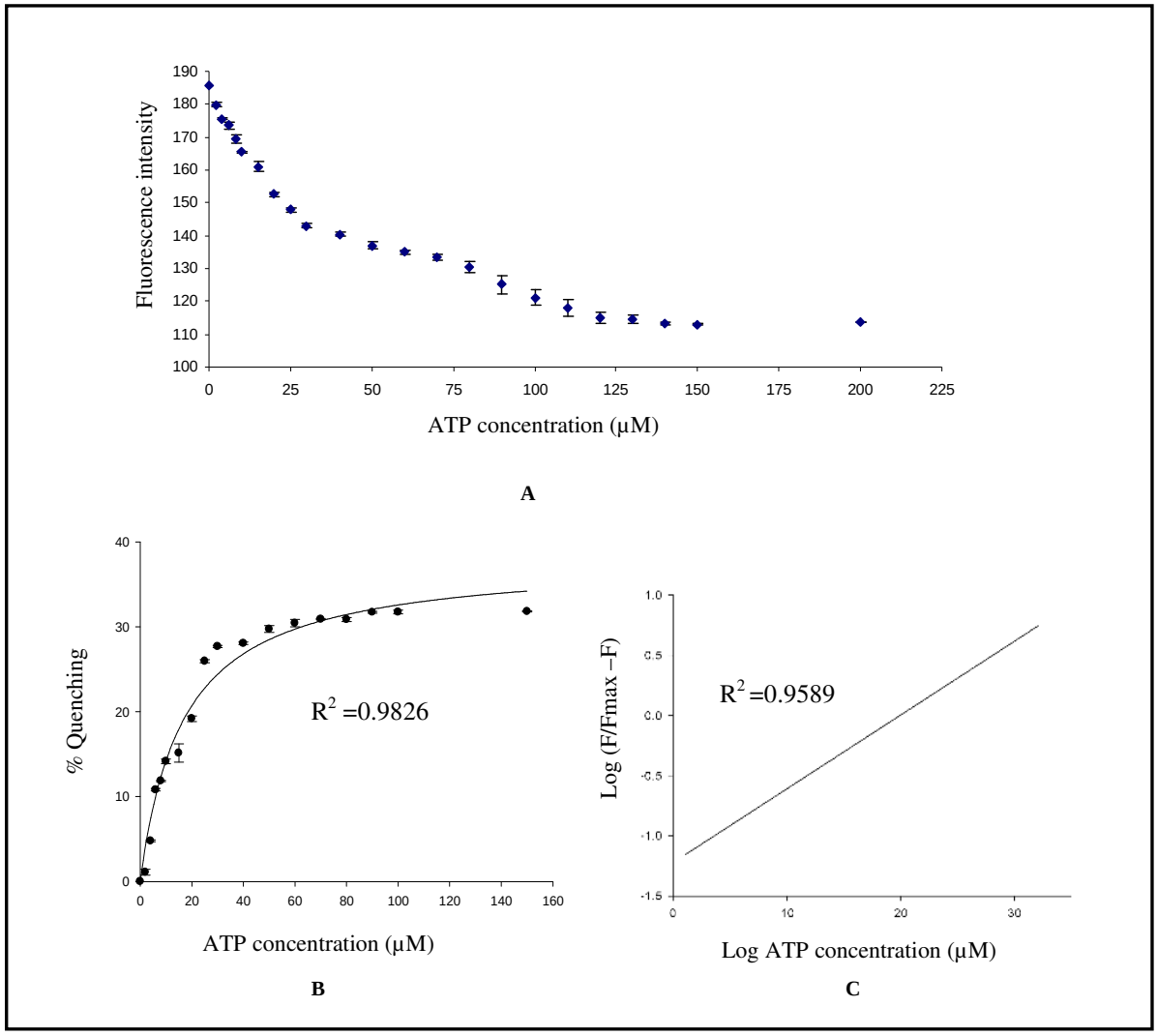

Figure 29: Quenching of basal rPDK4 fluorescence at 350 nm by ATP.

rPDK4 (5 µM) was excited at 295 nm and the fluorescence was measured at 350 nm.

The PDK proteins require Mg^{2+} for its activity (Tovar-Mendez *et al.*, 2005). In an event when $MgCl_2$ was not included in the buffer, ADP or ATP did not cause any quenching of basal fluorescence spectra rPDK4. Therefore, the observed quenching of fluorescence is due to specific binding of ATP or ADP by rPDK4.

4 Discussion

This research work focused on studying the structure of rPDK4 and further elucidating the binding properties of ADP to rPDK4. In order to achieve this aim, the study was divided into two sections. The first section involved utilization of computational methods to model the three dimensional structure of rPDK4. The modelled structure of rPDK4 was to study the hypothetical interaction between rPDK4 and ADP. The second section involved biochemical characterisation of the purified rPDK4 protein. This included size determination using size exclusion chromatography, SDS-PAGE and Western blot analysis, as well as kinase activity assays. The biochemical interaction of rPDK4 with ADP was studied using fluorescence quenching analysis.

4.1 Structural bioinformatics analysis of rPDK4

Analysis of the interaction of rPDK4 and the ADP molecule bound at the active site of the modelled rPDK4 revealed that amino acids Asn^{247}, Asp^{282}, Ser^{301}, Thr^{302}, Phe^{318} and Gly^{319} potentially make hydrogen bond interactions with the ADP molecule (Figure 15B). As described previously, these amino acids and their interactions appear to be conserved in all known isomers of PDK (Figure 5). This suggests that the binding mechanism of ADP is similar for all the isomers. This may increase the difficulty in designing active site inhibitors that would selectively bind rPDK4 and not the other PDK isomers since PDK4 has emerged as a potential drug target for the treatment of diabetes. Due to the conservation of the nucleotide binding domain of rPDK4 it is unlikely to be an ideal drug target, and specificity would be a major concern.

The first possible area of interest is the DCA binding site. Knoechel *et al*. (2006) studied the structure of human PDK2 in an attempt to find novel ligand binding sites that would be isoform specific. Taking into account that DCA has been shown to inhibit PDK activity by hindering dissociation of the ADP molecule at the active site (Bao *et al.*, 2004). Knoechel *et al*. (2006) undertook experiments to locate the DCA binding site. This site was successfully mapped (Figure 9). However, residues which constitute this site were also found to be conserved in all PDK isomers. Hence, it is unlikely that the DCA binding site will prove suitable as a drug target site for the development of inhibitors.

PDK dimers are recruited to the PDC by binding to the inner lipoyl (L2) domain of the E2 (Liu *et al.,* 1995). The L2 binding site could be another possible binding site that could be targeted. Tuganova *et al*. (2001) studied the interaction between the PDK isomers and L2 and showed that they display different binding affinities for L2 and this suggested that the L2 binding site in PDK could be different for each isomer. The findings of Tuganova *et al*. (2001) lead to the solving of the structure of human PDK3 complexed with L2 of PDC (Kato *et al*., 2005). It was observed from the structure of the PDK3-L2 complex that the L2 binds to PDK both at the N-terminal and C-terminal domains. The interactions between the N-terminal domain and L2 are mainly hydrophobic and electrostatic, and they are similar in all isomers of PDK based on sequence conservation. The tail of the C-terminal domain interacts with L2 through hydrogen bonding and the hydrogen bond network between the tail of C-terminal domain and L2 seems to be unique for each isomer (Kato e*t al.,* 2005). Furthermore, truncation of the C-terminal tail of PDKs abolishes the binding of L2 thus indicating that this region is crucial for L2 and PDK interaction (Kato *et al.,* 2005). The work of Kato *et al*. (2005)

indicates that the C-terminal tail region of PDK could be targeted for the design of PDK inhibitors that are isoform specific.

Another PDK ligand binding site that could be studied is that of the E1 subunit of PDC. It may lead to identification of isoform specific inhibitors of PDK because PDK isoforms are known to display differences in kinetic parameters, regulation and phosphorylation of E1 subunit (Bowker-Kinley *et al.,* 1998 and Kolobova *et al.,* 2001). It could also be worthy to target inactive PDK proteins as they may differ slightly in structure between isoforms. This approach has been employed successfully in designing Gleevec, a specific c-Abl kinase inhibitor which bind the inactive form of c-Abl kinase (Nagar *et al.,* 2003).

Hence, while the initial assumption that the ATP binding site could possibly be a suitable target site for the development of inhibitors appears to be incorrect, there are at least two other sites that can be targeted in future work.

4.2 The binding of ATP and ADP to rPDK4

ATP and ADP have been reported to bind PDK proteins at the active site (Steussy *et al.,* 2001 and Knoechel *et al.,* 2006). ATP, together with Mg^{2+} ions, is required for PDK activity (Tovar-Mendez *et al.,* 2002 and Tuganova *et al.,* 2001) while ADP inhibits the activity of PDK proteins (Pratt and Roche, 1979). To analyze the binding of ADP and ATP to rPDK4 proteins, fluorescence quenching was used.

Initial fluorescence work focused on determining basal fluorescence of rPDK4 in the absence of ATP and ADP. Excitation of tyrosine and tryptophan at 280 nm gives much

higher fluorescence intensity compared to a fluorescence intensity attained by exciting rPDK4 (tryptophan alone) at 295 nm (Figure 26). The difference in fluorescence emission wavelength when rPDK4 is excited at 280 than 295 nm is attributed to tyrosine and solvent inaccessible tryptophan residues which fluoresce at 280 nm.

Subsequently, rPDK4 was titrated with either ADP or ATP. Both ADP and ATP quenched the intrinsic fluorescence of rPDK4. The quenching of rPDK4 fluorescence by ADP and ATP was indicative of ADP and ATP binding to the active site. This was further supported by the inability of both ADP and ATP to quench Trp^{395} fluorescence in the absence of Mg^{2+} ions. The quenching of rPDK4 fluorescence by ADP and ATP also confirmed that Trp^{395} is sensitive to the binding of ADP and ATP to the rPDK4 nucleotide binding site. It could, therefore, be used to monitor the binding effects of ligands that target the nucleotide binding site.

The percentage quenching of rPDK4 basal fluorescence by ADP and ATP is shown in Figure 28B and Figure 29B, respectively. The maximum quenching effect of ATP and ADP are similar with values of 31 and 38 %, respectively. The Hill analysis of ADP and ATP binding yielded the n_H value 0.7 and 0.5, respectively. The obtained n_H value for both ADP and ATP is descriptive of cooperativity between the two binding sites. In an event where the n_H is less than 1 the cooperativity between the two sites is termed negative. This means that binding of ligand to one active site reduces the affinity of rPDK4 for the second ligand.

Hiromasa *et al*. (2006), when performing a similar experiment using human PDK2, obtained the n_H value of 1 for ADP. In this study, using PDK4 from rat, the n_H value of

0.7 was obtained. The n_H value of 1 describes non cooperativity between the two ADP binding sites implying that the two binding sites are independent and non interacting. The difference in the n_H value published by Hiromasa *et al*. (2006) and the one obtained in this study could be attributed to the use of different isomers of PDK which were from different sources.

The Hill analysis of ATP obtained in this work was compared to that of Hiromasa *et al*. (2006). It was observed that both n_H value describe a negative cooperativity between the two ATP binding sites. However, a n_H value of 0.5 obtained in this work shows that the two ATP binding sites in rPDK4 have stronger negative cooperativity than those in human PDK2 since they gave an n_H value of 0.9 which is closer to 1.

Taking into consideration that ATP activates PDK activity and PDK functions as a dimer, one would assume that the two binding sites of ATP exhibit positive cooperativity. This would mean that the binding of ATP to one monomer of PDK would increase the affinity of the other monomer to bind an ATP molecule. However, this seems to be untrue for the case of PDKs. Consequently, the n_H of 0.5 for ATP was unanticipated.

The K_d value of 37 μM for ADP and 17.4 μM for ATP obtained in this study illustrates that rPDK4 has higher affinity for ATP than for ADP. This result is consistent with published work of Hiromosa *et al*. (2006) and Bao *et al*. (2004). It was anticipated for ATP to have a higher affinity than ADP, since ATP is required for the catalysis of PDK. The moderate affinity binding of ATP will also greatly favour the exchange of ADP for ATP molecule to prevent PDK inhibition by ADP.

In order to design inhibitors that would effectively inhibit rPDK4 one has to take into account the high binding affinity of ATP for PDK. Drug leads need to have a greater affinity for nucleotide binding site on PDK and out compete ATP binding. While it may be worthy to design drugs that target the active site, the candidates that target the pyruvate binding site may be a worthwhile investigation since they have been shown to work synergistically with ADP. Pyruvate binding has been successfully mapped using DCA, a structural analog of pyruvate. The binding of DCA or pyruvate is reported to induce conformational changes that prevent dissociation of ADP from the active site thus locking ADP in the active site of PDK (Bao *et al.,* 2004).

4.3 Conclusions and future work

Rat PDK4 has been successfully expressed and purified. It was found to be active and binds both ATP and ADP. This provides a good platform for future work in designing inhibitors that target the active site of this protein. The structural analysis of the ADP binding site in this work has shown the disadvantages of designing drugs that target the active site. It is important to design drug leads that would target other ligand binding sites such as the E1 and L2 binding sites on PDK.

This work has also shown that Trp^{395} can successfully used to study the effects of ligands that bind to the PDK active site. The presence of another tryptophan residue (Trp^{81}) in PDKs (is located near the DCA binding site) could be exploited to studying the interaction between rPDK4 and DCA or other PDK inhibitors that target the DCA binding site using tryptophan fluorescence. As yet, monitoring of the interaction of PDK and DCA using tryptophan fluorescence does not appear to have been investigated.

5 References

Aicher, T.D., Damon, R. E., Koletar, J. Vinluan, C.C., Brand, L.J., Gao, J., Shetty, S.C., Kaplan E.L. and Mann, W.R (1999) Triterpene and diterpene inhibitors of pyruvate dehydrogenase kinase. Bioorg. Med. Chem. Lett. **9**, 2223-2228.

Alex, L.A. and Simon, M.I. (1994) Protein histidine kinases and signal transduction in prokaryotes and eukaryotes. Trends Genet. **10**, 133–138.

Altschul, S.F., Madden T. L., Schaffer, A.A., Zhang Z., Miller, W. and Lipman D.J (1997) Gapped BLAST and PSI-BLAST: a new generation of protein database search programs. Nucleic Acid Res. **25**, 3389-3402.

Amos, A.F., McCarthy, D.J. and Zimmet, P. (1997) The rising global burden of diabetes and its complications: estimates and projections to the year 2010. Diabet. Med. **5**, 81-85.

Baker, A.J., Gibson, K.H., Grundy, W., Godfrey, A.A, Barlow, J.J., Healy, M.P., Woodburn, J.R., Ashton, S.E., Curry, B.J., Scarlett, L., Henthorn, L. and Richards, L. (2001) Studies leading to the identification of ZD1839 (Irressa): an orally active, selective epidermal growth factor receptor tyrosine kinase inhibitor targeted to the treatment of cancer. Bioorg. Med. Chem. Lett. **11**, 1911-1914.

Bao, H., Kasten, S.A, Yan, X., and Roche, T.E. (2004) Pyruvate dehydrogenase kinase isorform 2 activity limited and further inhibited by slowing down the rate of dissociation of ADP. Biochemistry **43**, 13432-13441.

Bergerat, A., de Massy, B., Gadelle, D., Varoutas, P.C., Nicolas, A. and Forterre, P. (1997) An atypical topoisomerase II from Archaea with implications for meiotic recombination. Nature **386**, 414–417.

Bersin, R.M. and Stacpoole, P.W. (1997) Dichloroacetate as metabolic therapy for myocardial ischemia and failure. Am. Heart J. **13**, 841-855.

Bilwes A.M., Alex, L.A., Crane, B.R. and Simon, M.I. (1999) Structure of CheA, a signal-transducing histidine kinase. Cell **96**, 131–141.

Bilwes A.M., Quezada, C.M., Croal, L.R., Crane, B.R. and Simon, M.I. (2001) Nucleotide binding by the histidine kinase CheA. Nature Struct. Biol. **8**, 353–360.

Bowker-Kinley, M.M and Popov, K.M. (1999) Evidence that pyruvate dehydrogenase kinase belongs to the ATPase/kinase superfamily. Biochem. J. **344**, 47-53.

Bowker-Kinley, M.M., Davis, W.I., Wu, P., Harris, R.A., and Popov, K.M. (1998) Evidence for existence of tissue-specific regulation of the mammalian pyruvate dehydrogenase complex. Biochem. J. **329**, 191-196.

Brenner, S.E. (2001) A tour of structural genomics. Nature Rev. Genet. **2**, 801–809.

Coleman, R.A., Winter, H.S. and Wolf, B. (1992) Glycogen storage disease type III (glycogen debranching enzyme deficiency): correlation of biochemical defects with myopathy and cardiomyopathy. Ann. Intern. Med. **116**, 896-900.

Cooper, R.H., Randle, P.J. and Denton, R.M. (1975) Stimulation of phosphorylation and inactivation of pyruvate dehydrogenase by physiological inhibitors of the pyruvate dehydrogenase reaction. Nature **275**, 808–809.

Corbett, K.D. and Berger, J.M. (2003) Structure of the topoisomeraseVI-B subunit: implications for type II topoisomerase mechanism and evolution. EMBO J. **22,** 151-163.

Dahl, H.H., Hunt, S.M., Huttchison, W.M. and Brown, G.K. (1987) The human pyruvate dehydrogenase complex. Isolation of cDNA clones for the E1 alpha subunit, sequence analysis, and characterisation of the mRNA. J. Biol. Chem. **15**, 7398-7403.

Davier, J. R., Wynn, R.M., Meng, M., Huang, Y.S., Aalund, G, Chaung, D.T., and Lau, K. S. (1995) Expression and characterisation of branched-chain alpha-ketoacid dehydrogenase kinase from rat. Is it a histidine kinase? J. Biol. Chem. **270**, 19861-19867.

Dennis, S.C., Debuyser, M., Scholz, R. and Olson, M.S. (1978) Studies on the relationship between ketogenesis and pyruvate oxidation in isolated rat liver mitochondria. J. Biol. Chem. **253**, 2229-2237.

Denyer, G.S., Lam, D., Cooney, G.J. and Catrson, I.D. (1981) Effect of starvation and insulin in vivo on the activity of the pyruvate dehydrogenase complex in rat skeletal muscle. FEBS Lett. **250**, 464-468.

Gudi, R., Bowler-Kinley, M.M., Kedishvili, N.Y., Zhao, Y. and Popov, K.M. (1995) Diversity of the pyruvate dehydrogenase gene family in humans. J. Biol. Chem. **270**, 28989-28994.

Guex, N. and Peitsch, M.C. (1997) SWISS MODEL and the Swiss-PDBViewer: An environment for comparative protein modelling. Electrophoresis **18**, 2714-2723.

Hanks, S.K. and Hunter, T. (1995) The eukaryotic protein kinase superfamily: kinase (catalytic) domain structure and classification. FASEB J. **9**, 576–596.

Harris, R.A., Popov, K.M., Zhao, Y., Kedishvilli, N.Y., Shimomura, Y. and Crabb, D.W. (1995) A new family of protein kinases- The mitochondrial protein kinases. Advan. Enzyme Regul. **35**, 147-162.

Hawkes, C. and Kar, S. (2002) Insulin-like growth factor-II/Mannose-6-phosphate receptor in the spinal cord and dorsal root ganglia of the adult rat. Eur. J. Neurosci. **15**, 1-33.

Henry, R.R., Thornburn, A.W., Beerdson, P. and Gubiner, B. (1991) Dose-response characteristics of impaired glucose oxidation in non-insulin-dependent diabetes mellitus. Am. J. Physiol. **261**, E132-E140.

Hiromasa, Y., Hu, L. and Roche, T.E. (2006) Ligand –induced effects on pyruvate dehydrogenase kinase isoform 2. J. Biol. Chem. **281,**12568-12579

Holness, M.J. and Sugden, M.C. (1989) Pyruvate dehydrogenase activites during fed-to-starved transition and re-feeding after acute or prolonged starvation. Biochem. J. **258**, 529-533.

Holness, M.J., Kraus, A., Harris, R.A. and Sugden, M.C. (2000) Targeted upregulation of pyruvate dehydrogenase kinase (PDK)-4 in slow-twitch skeletal muscle underlies the stable modification of the regulatory characteristics of PDK induced by high-fat feeding. Diabetes **49**, 775-781.

Huang, B., Gudi, R., Wu, P., Harris, R.A, Hamilton, J. and Popov, K.M. (1998) Isoenzymes of pyruvate dehydrogenase phosphatase. DNA-derived amino acid sequences, expression, and regulation. J. Biol. Chem. **273**, 17680-17688.

Huang, B., Wu, P.,Gudi, Popov, K.M and Harris, R.A, (2000) Regulation of pyruvate dehydrogenase kinase expression by proliferator-activated receptor –α ligands , glucocorticoids, and insulin. Diabetes **51,** 276-283.

Hucho, F., Randall, D.D., Roche, T.E., Burgett, M.W., Pelley, J. W., and Reed, L.J. (1972) α Keto acid dehydrogenase complexes. XVII. Kinetic and regulatory properties of pyruvate dehydrogenase kinase and pyruvate dehydrogenase phosphotase from bovine kidney and heart. Arch. Biochem. Biophys. **151**, 328-340.

Huse, M. and Kuriyan, J. (2002) The conformational plasticity of protein kinases. Cell **109**, 275-282.

Jackson, J.C., Vinluan, C.C., Dragland, C.J., Sundrararajan, V., Yan, B., Gounnarides, J.S., Nirmala, N.R., Topoil, S., Ramage, P., Blume, J.E., Aicher, T.D., Bell, P.A., Mann, W.R. (1998). Heterologously expressed inner lipoyl domain of dihydrolypoly acetyltransferase inhibits ATP-dependent inactivation of pyruvate

dehydrogenase complex. Identification of important amino acid residues. Biochem. J. **334**, 703-711.

Kahn, B.B. and Flier, J.S. (2000) Obesity and insulin resistance. J. Clin. Invest. **106,** 473-481.

Kato, M., Chuang, J. L., Tso, S., Wynn, R.M. and Chuang, D. T. (2005) Crystal structure of pyruvate dehydrogenase kinase bound to lipol domain 2 of human pyruvate dehydrogenase complex. EMBO J. **24**, 1763-1774.

Katz, R., Tai, C.N., Diener, R.M., McConnell, R.F. and Semonick, D.E. (1981) Dichloroacetate sodium: 3-month oral toxicity studies in rats and dogs. Toxicol. Appl. Pharmacol. **57**, 273-287.

Kerbey, A.L. and Randle, P.J. (1982) Pyruvate dehydrogenase kinase/activator in rat heart mitochondria, Assay, effect of starvation, and effect of protein-synthesis inhibitors of starvation. Biochem. J. **206**, 101-111.

Kim, D. and Forst, S. (2001) Genomic analysis of the histidine kinase family in bacteria and archaea. Microbiology **147**, 1197-1212.

Knoechel, T.R, Tucker, A.D., Robinson, C.M., Philips, C. Wendy, T., Bungay, P.J., Kasten, S.A, Roche, T. E., and Brown, D.G. (2006) Regulatory roles of the N-terminal based on crystal structures of human pyruvate dehydrogenase kinase 2 containing physiological and synthetic ligand. Biochemistry **45**, 402-415.

Kolobova, E., Tuganova, A., Boulatnikov, I. and Popov, K.M. (2001) Regulation of pyruvate dehydrogenase activity through phosphorylation at multiple sites. Biochem. J. **358**, 69077-69082.

Korc, M. (2003). Diabetes mellitus in the era of proteomics. Mol. Cell. Proteomics **26**, 399-404.

Kopelman, P.G. and Hitman, G.A. (1998) Diabetes. Exploding type II. Lancet **352**, 19-26.

Korotchkina, L.G. and Patel, M.S. (1995) Mutagenesis studies of the phosphorylation sites of recombinant human pyruvate dehydrogenase. Site-specific regulation. J. Biol. Chem. **270**, 14297−14304.

Korotchkina, L.G. and Patel, M.S. (2001) Site specificity of four pyruvate dehydrogenase kinase isoenzymes toward the three phosphorylation sites of human pyruvate dehydrogenase. J. Biol. Chem. **276**, 37223-37229.

Laemmli, U.K. (1970) Cleavage of structural proteins during the assembly of the head of bacteriophage T4. Nature **227**, 680-685.

Liu. S., Baker, J.C., and Roche, T.E. (1995) Binding of the pyruvate dehydrogenase kinase to recombinant constructs containing the inner lipoyl domain of the dihydrolipoyl acetyltransferase component. J. Biol. Chem. **270**, 793−800.

Machius, M., Chuang, J.L., Wynn, R.M., Tomchick, D.R. and Chuang, D.T. (2001) Structure of rat BCKD kinase: nucleotide-induced domain communication in a mitochondrial protein kinase. Proc. Natl. Acad. Sci. USA **98**, 11218–11223.

Maiti, R., Domselaar, G.H., Zhang, H. and Wishart, D.S. (2004) Superpose: a simpler server for sophisticated structural superposition. Nucleic Acids Res. **32,** 590-594.

Majer, M., Popov, K.M., Harris, R.A., Bogardus, C., and Prochazka, M. (1998) Insulin down-regulates pyruvate dehydrogenase kinase (PDK) mRNA: potential mechanism contributing to increased lipid oxidation in insulin-resistant subjects. Mol. Genet. Metab. **65**, 181-186.

Mann, R.W., Dragland, J.C., Vinluan, C.C., Vedananda, P.A., Bell, P.A., Aicher T.D. (2000) Diverse mechanisms of inhibition of pyruvate dehydrogenase kinase by structurally distinct inhibitors. Biochim. Biophys. Acta. **1480**, 283-292.

Mohammadi, M., McMahon, G., Sun, L., Tang, C., Hirth, P., Yeh, B.K., Hubbard, S.R. and Schlessinger, J. (1997) Structures of the tyrosine kinase domain of fibroblast growth factor receptor in complex with inhibitors. Science **276**, 955-959.

Mooney, B. P., David, N. R., Thelen, J. J., Miernyk, J. A. and Randall, D.D. (2000) Histidine Modifying Agents Abolish Pyruvate Dehydrogenase Kinase Activity. Biochem. Biophys. Res. Commun. **267**, 500-504.

Nagar, B., Hantschel, O., Young, M.A., Scheffezek, K., Veach, D., Bornmarnn, W., Clarkson, B., Superti-Furga, G. and Kuriyan, J. (2003) Structural basis for the autoinhibition of c-Abl tyrosine kinase. Cell **122**, 859-871.

Noble, M.E., Endicott, J.A. and Johnson, L.N. (2004) Protein kinase inhibitors: insights into drug design from structure. Science **19**, 1800-1805.

Pargellis, C., Tong, L., Churchill, L., Cirillo, P.F., Gilmore, T., Graham, A.G., Grob, P.M., Hickey, E.R., Moss, N., Pav, S. and Regan, J. (2002) Inhibition of p38 MAP kinase by utilizing a novel allosteric binding site. Nat. Struct. Biol. **9**, 268–272.

Parkinson, J.S. and Kofoid E.C. (1992) Communication models in bacterial signalling proteins. Annu. Rev. Genet. **26**, 71-112.

Patel, M.S. and Korotchkina, L.G. (2001) Regulation of mammalian pyruvate dehydrogenase complex by phosphorylation: complexity of multiple phosphorylation sites and kinases. Exp. Mol. Med. **4**, 191-197.

Patel, M.S. and Roche, T.E. (1990) Molecular biology and biochemistry of pyruvate dehydrogenase complexes. FASEB J. **4**, 3224-3233.

Pearson, W.R. (1990) Rapid and Sensitive Sequence Comparison with FASTP and FASTA. Meth. Enzymol. **183**, 63-98.

Popov, K.M., Kedishvili, N.Y., Zhao, Y., Gudi, R. and Harris, R.A. (1994) Molecular cloning of the p45 subunit of pyruvate dehydrogenase kinase. J. Biol. Chem. **269**, 29720-29724.

Popov, K.M., Kedishvili, N.Y., Zhao, Y., Shimomura, Y., Crabb, D.W. and Harris, R.A. (1993) Primary structure of pyruvate dehydrogenase kinase establishes a new family of eukaryotic protein kinases. J. Biol. Chem. **268**, 26602-26606.

Prade, L., Engh, R.A., Girod, A., Kinzel, V., Huber, R., and Bossemeyer, D. (1997) Staurosporine-induced conformational changes of cAMP-dependent protein kinase catalytic subunit explain inhibitory potential. Structure **15**, 1627-1637.

Pratt, M.L. and Roche, T.E. (1979) Mechanism of pyruvate inhibition of kidney pyruvate dehydrogenase kinase and inhibitory by pyruvate and ADP. J. Biol. Chem. **254**, 7191-7196.

Preiser, J.C., Moulart, D. and Vincent, J.L. (1990) Dichloroacetate administration in the treatment of endotoxic shock. Circ. Shock **30**, 221-228.

Prodromou, C., Roe, S.M., O'Brien, R., Ladbury, J.E., Piper, P.W., and Pearl, L.H. (1997) Identification and structural characterisation of the ATP/ADP binding site in the Hsp90 molecular chaperone. Cell **90**, 65-75.

Ramachandran, G. N. and Sasiskharan, V. (1968) Conformation of polypeptides and proteins. Adv. Protein Chem. **23**, 283-437.

Randle, P.J. (1986) Fuel sensing in animals. Biochem. Soc. Trans. **14**, 799-806.

Ravindran, S., Randke, G.A., Guest, J.R., and Roche, T.E. (1996) Lipoyl domain-based mechanism for the integrated feedback control of the pyruvate dehydrogenase complex by enhancement of pyruvate dehydrogenase kinase activity. J. Biol. Chem. **271**, 653-662.

Reed, L.J., Dumuni, Z. and Merryfleid, M.L. (1985) Regulation of mammalian pyruvate and branched-chain α-keto acid dehydrogenase complexes by phosphorylation – dephosphorylation. Curr. Opin. Cell Regul. **27**, 41-49.

Rossman, M.G., Moras, D. and Olsen, K.W. (1974) Chemical and biological evolution of nucleotide-binding protein. Nature **250**, 194-199.

Rowles, J.C., Scherer, S.W., Xi, T., Majer, M., Nickle, D.C., Rommens, J.M., Popov, K.M., Harris, R.A., Riebow, N.L., and Xia, J. (1996) Cloning and characterisation of PDK4 on 7q21.3 encoding a fourth pyruvate dehydrogenase kinase isoenzyme in human. J. Biol. Chem. **271**, 22376-22382.

Sale, G.J. and Randle, P.J. (1981) Occupancy of sites of phosphorylation in inactive rat heart pyruvate dehydrogenase phosphate in vivo. Biochem. J. **193**, 3935–946.

Schulz, G.E., Schiltz, E., Tomassellu, A.G., Frank, R., Brune, M., Witting-hofer, A. and Schirmer, R.H. (1986) Structural relationship in the adenylate kinase family. Eur. J. Biochem. **161**, 127-132.

Schwede, T., Kopp, J., Guex, N. and Pietsch, M.C. (2003) Swiss- model: an automated protein homology modelling server. Nucleic Acids Res. **31**, 3381-3385.

Siess, E.A. and Wieland, O.H. (1976). Phosphorylation state of cytosolic and mitochondrial adenine nucleotides and of pyruvate dehydrogenase in isolated rat liver cells. Biochem. J. **156,** 91–102.

Stacpoole, P.W., Harwood H.J., Cameron, D.F., Curry, S.H., Samuelson, D.A., Cornwell, P.E. and Sauberlich, H.E. (1990) Chronic toxicity of dichloroacetate: possible relation to thiamine deficiency in rats. Fundam. Appl. Toxicol. **14**, 327-337.

Stacpoole, P.W., Moore, G.W. and Kornhauser, D.M. (1979) Toxicity of chronic dichloroacetate. N. Engl. J. Med. **300**, 372-376.

Steussy, C.N., Popov, K.M., Bowker-Kinley, M.M., Soan, R.B., Harris, R.A. and Hamilton, J.A. (2001) Structure of pyruvate dehydrogenase kinase: Novel folding pattern for a seine protein kinase. J. Biol. Chem. **276**, 37443-37450.

Sugden, M.C., Bulmer, K., Augustine, D. and Holness, M.J. (2001) Selective modification of pyruvate dehydrogenase isoform expression in rat pancreatic islets elicited by starvation and activation of peroxisome proliferator-activated receptor-α. Diabetes **50**, 2729-2736.

Sugden, M.C., Fryer, L.G., Orfali, K.A., Priestman, D.A., Donald, E. and Holness, M.J. (1998) Studies of the long-term regulation of hepatic pyruvate dehydrogenase kinase. Biochem. J. **329**, 89-94.

Sugden, M.C., Kraus, A., Harris, R.A. and Holness, M.J. (2000) Expression and regulation of pyruvate dehydrogenase kinase isoforms in the developing rat heart and in adulthood: role of thyroid hormone status and lipid supply. Biochem. J. **346**, 651-657.

Tanaka, T., Saha, S.K., Tomomori, C., Ishima, R., Liu, D., Tong, K.I., Park, H., Dutta, R., Qin, L., Swindells, M.B., Yamazaki, T., Ono, A.M., Kainosho, M., Inouye, M. and Ikura, M. (1998) NMR structure of the histidine kinase domain of the *E. coli* osmosensor EnvZ. Nature **396**, 88–92.

Teague, W.M., Pettit, F.H., Yeaman, S.J. and Reed L.J. (1979) Function of phosphorylation sites on pyruvate dehydrogenase. Biochem. Biophys. Res. Commun. **87**, 651-657.

Thelen, J.J. Miernyk, J.A. and Randall, D.D. (2000) Pyruvate dehydrogenase kinase from *Arabidopsis thaliana*: a protein histidine kinase that phosphorylate serine residue. Biochem. J. **349**,195-201.

Thompson, J.D., Higgins, D.G. and Gibson, T.J. (1994) CLUSTAL W: improving the sensitivity of progressive multiple sequence alignment through sequence weighting,

position-specific gap penalties and weight matrix choice. Nucleic Acids Res. **22,** 4673-4680.

Toth, G.P., Kelty, K.C., George, E., Read, E.J. and Smith, M.K. (1992) Adverse male reproductive effects following subchronic exposure of rats to sodium dichloroacetate. Fundam. Appl. Toxicol. **19**, 57-63.

Tovar-Mendez, A., Hirani, T.A., Miernyk, J.A., Randall, D.D. (2005) Analysis of the catalytic mechanism of pyruvate dehydrogenase kinase. Arch. Biochem. Biophys. **434**,159-168.

Tuganova, A. Yoder, M.D. and Popov, K.M. (2001) An essential role of Glu-243 and His-239 in the phosphotransfer reaction catalyzed by pyruvate dehydrogenase kinase. J. Biol. Chem. **276**, 17994-17999.

Vriend, G. (1990) WHAT IF: A molecular modelling and drug design program. J. Mol. Graph **8**, 52-56.

Whitehead, J.P., Clark, S.F., Urso, B. and James, D.E. (2000) Signalling through the insulin receptor. Curr. Opin. Cell Biol. **12**, 222-228.

Whitehouse, S., Cooper, R.H. and Randle, P.J. (1974) Mechanism of activation of pyruvate dehydrogenase by dichloroacetate and other halogenated carboxylic acids. Biochem. J. **141**,761-777.

Wieland, O., Siess, E. Schulze-Wethmar, F.H., von Funcke, H.G. and Winton, B. (1971) Active and inactive forms of pyruvate dehydrogenase in rat heart and kidney: Effect of diabetes, fasting, and refeeding on pyruvate dehydrogenase interconversion. Arch. Biochem. Biophys. **143**, 593-601.

Wu, P., Inskeep, K., Bowker-Kinley, M.M., Popov, K.M. and Harris, R.A. (1999) Mechanism responsible for the inactivation of skeletal muscle pyruvate dehydrogenase complex in starvation and diabetes. Diabetes **48**, 1593-1599.

Wu, P., Sato, J., Zhao, Y., Jaskiewicz, J., Popov, K.M. and Harris, R.A. (1998) Starvation and diabetes increase the amount of pyruvate dehydrogenase kinase isoenzyme 4 in rat heart. Biochem. J. **329**, 197-201.

Yeaman, S.J., Hutcheson, E.T., Roche, T.E., Pettit, F.G., Brown, J.R., Reed, L.J., Watson, D.C, and Dixon, G.H. (1978) Sites of phosphorylation on pyruvate dehydrogenase from bovine kidney and heart. Biochemistry **17**, 2364-2370.

Yount, E.A., Felten, S.Y., O'Connor, B.L., Eterson, R.G., Powel, R.S., Yum, M.N. and Harris, R.A. (1982) Comparison of the metabolic and toxic effects of 2-choloropropionate and dichloroacetate. J. Pharmacol. Exp. Ther. **222**, 501-508.

Zierath, J.R., He, L., Guma, A., Odegoard, W. E., Klip, A. and Wallberg-Henriksson H. (1996) Insulin action on glucose transport and plasma membrane GLUT4 content in skeletal muscle from patients with NIDDM. Diabetologia. **39**, 1180-1189.